

Design of a Micro Aerial Vehicle

A Major Qualifying Project Report

Submitted to the Faculty of the

WORCESTER POLYTECHNIC INSTITUTE

In Partial Fulfillment of the Requirements for the

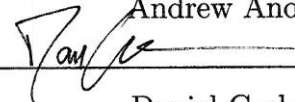
Degree of Bachelor of Science

in Aerospace Engineering

Submitted by:



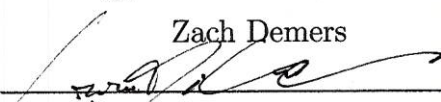
Andrew Andraka



Daniel Cashman



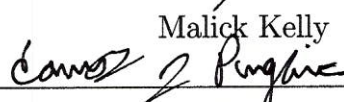
Zach Demers



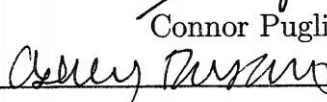
Giovanni Di Cristina



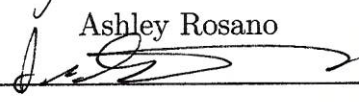
Malick Kelly



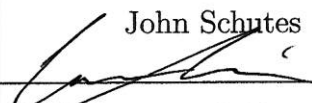
Connor Pugliese



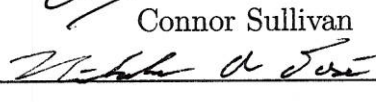
Ashley Rosano



John Schutes



Connor Sullivan



Nicholas Tosi

30 April 2015

Approved by:



Professors: Anthony B. Linn & Seong-Kyun Im, Advisors

Aerospace Engineering Program

Mechanical Engineering Department, WPI

Abstract

An unmanned aerial vehicle was designed and built for the AIAA Design Build Fly 2015 competition. To meet the mission requirements, including speed and weight, the aircraft is designed to have a 10-foot wingspan and 14 inch chord with dihedral and a conventional tail wing configuration. To minimize the weight without durability cost, tubular carbon fiber spars and balsa ribs were used to construct the wings. The 5-foot fuselage consists of bulkheads made from balsa ply connected longitudinally by carbon fiber tubes. An 18 inch diameter propeller driven by a brushless DC motor generates the thrust. The aircraft has a 5 pound payload capability. By combining detailed analysis of aerodynamics, structure, and material with flight test, the team has refined the aircraft design.

Certain materials are included under the fair use exemption of the U.S. Copyright Law and have been prepared according to the fair use guidelines and are restricted from further use.

Acknowledgments

The team would like to thank our advisors, Professors Anthony B. Linn and Seong-Kyun Im for their guidance and support, the employees at Turn4Hobbies for their assistance in parts ordering and acquisition, the AIAA Massachusetts Chapter for their generous financial support, the Aerospace Engineering program for providing lab space and tools, and finally to Barbara Fuhrman and Donna Hughes for assisting us with our logistical problems.

Authorship

Section	Contributor
Introduction	GDC, AR, ZD
Conceptual Design	
Mission Requirements	GDC, AR
Mission to Design Requirements	GDC, AR
Solutions Considered, Selection Process, Results	GDC, AR
Preliminary Design	
Design Methodology	ZD, NT
Drop Mechanism	MK
Sizing and Trade Studies	GDC, ZD
Mission Model	ZD
Aircraft Characteristics	NT, GDC, ZD, DC, CS
Preliminary Mission Performance	DC, NT
Detail Design	
Dimension and Parameters	CS
Structural Characteristics	DC
Subsystem Design	AA, MK, CS, NT
Weight and Balance	DC, ZD
Performance Parameters	DC, NT
Drawing Package	DC, ZD, MK
Manufacturing Plan	
Process and Techniques	MK, JS
Wing Construction	MK
Fuselage Construction	MK
Electrical System	ZD
Manufacturing Gantt and Milestone Chart	MK
Testing Plan	
Flight Testing	AA, MK
Drop Mechanism Testing	MK
Structural Tests	ZD
Aerodynamic and Propulsion Tests	GDC
Controls and Avionics	MK
Battery Tests	ZD
Performance Results	
Structural Tests	MK, CS
Control Test	MK
Competition Results	DC
Recommendations for future work	NT
Report Editing	AA, DC, ZD, GDC, MK, AR, JS, CS, NT
Report Formatting	GDC

Contents

List of Figures	6
1 Introduction	8
2 Conceptual Design	10
2.1 Mission Requirements	10
2.1.1 Mission and Scoring Summary	10
2.1.2 Flight Course	11
2.1.3 Ground Mission–Payload Loading Time	12
2.1.4 Flight Mission 1–Ferry Flight	12
2.1.5 Flight Mission 2–Sensor Package Transport	13
2.1.6 Flight Mission 3–Sensor Drop	14
2.2 Mission to Design Requirements	15
2.2.1 Sensitivity Analysis	15
2.2.2 Design Constraints	17
2.2.3 Design Requirements	18
2.2.4 Battery Selection	19
2.3 Solutions Considered, Selection Process, Results	20
2.3.1 General Configuration	21
2.3.2 Wing Configuration	22
2.3.3 Motor Configuration	22
2.3.4 Landing Gear Configuration	23
2.3.5 Tail Configuration	24
3 Preliminary Design	26
3.1 Design Methodology	26
3.1.1 Wings	26
3.1.2 Fuselage	26
3.1.3 Empennage	27
3.1.4 Propulsion	27

3.2	Drop Mechanism	27
3.3	Sizing and Trade Studies	30
3.4	Mission Model	31
3.5	Aircraft Characteristics	32
3.5.1	Final Airfoil Selection Analysis	32
3.5.2	Drag Estimate	36
3.5.3	Stability and Control	38
3.5.4	Structural Design	42
3.6	Preliminary Mission Performance	45
4	Detail Design	47
4.1	Dimensions and Parameters	47
4.2	Structural Characteristics	48
4.2.1	Fuselage	48
4.3	Subsystems Design	50
4.3.1	Propulsion	50
4.3.2	Controls	52
4.3.3	Landing Gear	53
4.3.4	Payload	55
4.3.5	Drop Mechanism	55
4.4	Weight & Balance	56
4.5	Performance Parameters	58
5	Manufacturing	59
5.1	Process and Techniques	59
5.1.1	Laser Cutting	59
5.1.2	Balsa Ply Construction	60
5.1.3	Carbon Fiber Tubing	60
5.1.4	Carbon Fiber Wet Laying	61
5.1.5	Sheet Metal Forming	62
5.1.6	Ultracoating	63
5.2	Wing Construction	64
5.2.1	Wing sub-assemblies	64
5.2.2	Dihedral Boxes	65
5.2.3	Thermoform Plastic Cover	66

5.3	Fuselage Construction	66
5.4	Electrical System	69
5.5	Manufacturing Gantt and Milestone Chart	70
6	Testing	71
6.1	Flight Testing	71
6.1.1	Site location and Static Testing	71
6.1.2	Initial Flight Test hops	72
6.1.3	Initial Flight Test	74
6.1.4	Mission Flight Testing	74
6.2	Drop Mechanism Testing	76
6.3	Structural Tests	76
6.4	Aerodynamic & Propulsion Tests	77
6.5	Controls & Avionics	77
6.6	Battery Tests	78
7	Performance Results	79
7.1	Structural Tests	79
7.1.1	Wing Torsion Test	79
7.1.2	Static Load Test	79
7.1.3	Dihedral Box Test	80
7.1.4	Landing Gear Weight Test	80
7.1.5	Fuselage Twist Test	81
7.2	Controls Test	81
7.3	Competition Results	81
8	Recommendations for future work	84
9	References	87
	Appendix A Drawing Package	88
	Appendix B Org Chart	94

List of Figures

2.1	Flight Course	11
2.2	Flight Mission 2 Payload	13
2.3	Flight Mission 3 Payload	14
2.4	Flight Mission 3 Drop Zone	15
2.5	Scoring Sensitivity Analysis	17
2.6	General Configuration	21
2.7	Motor Configuration	23
2.8	Landing Gear Configuration	24
2.9	Tail Configuration	25
3.1	Ratchet Mechanism	29
3.2	Drop Mechanism Camshaft	30
3.3	Cl v Cd of NACA 4412	33
3.4	Cl v AoA for NACA 4412	33
3.5	Cl v AoA for Decreased Airfoil Thickness	34
3.6	Cl v AoA for Increased Airfoil Camber	35
3.7	Cl v Cd for Varying Airfoil Camber, Teal-4%, Green-8%	36
3.8	Aircraft Component Coefficient of Drag	37
3.9	Aircraft Drag Buildup Percentages	37
3.10	Munk’s Diagram	38
3.11	Aerodynamic Center Calculations	39
3.12	Stability Derivatives	40
3.13	NACA 0012 tail airfoil analysis	41
3.14	Wing Structure	43
3.15	Fuselage Model	44
3.16	Fuselage Trussing	45
3.17	Mission Evaluation	46
3.18	Mission Analysis	46
4.1	Wing and Fuselage Dimensions	47

4.2	Tail Dimensions	47
4.3	Battery and Motor Dimensions	48
4.4	Fuselage Structure	49
4.5	Aircraft Weight Estimate	50
4.6	Preliminary Motor Selection	51
4.7	Final Landing Gear Configuration	54
4.8	Weight and Balance	57
4.9	Performance Parameters	58
5.1	Wet Carbon Fiber	62
5.2	Coating the fuselage	63
5.3	D-cell forming.	65
5.4	Fuselage Construction Process	68
5.5	Manufacturing Gantt and Milestone Chart	70
6.1	Damage Sustained during hops	73
6.2	Test Flight	75
6.3	Structural Test	77
7.1	Static Load test during flight testing.	80
7.2	Malick, Andrew, Zach, and Dan at the DBF Competition	82
B.1	Team Organizational Chart	94

Introduction

The purpose of this project was to design, manufacture, and test an aircraft entry into the 2014-15 American Institute of Aeronautics and Astronautics/Cessna/Raytheon Design/Build/Fly (AIAA DBF) competition. The overall objective of the competition is to design an electric-powered, remote controlled aircraft capable of completing a mission matrix. To do this, the team needed to apply knowledge of aerodynamics, structural mechanics, stability, and engineering design and testing.

The AIAA DBF provided a conflicting set of design parameters that needed to be optimized in order to obtain the highest possible score. These parameters included speed of flight, aircraft empty weight, ability of the aircraft to carry a large payload, and complexity. These design parameters were tested over the course of four different missions: one ground mission and three flight missions. The ground mission is a measure of how quickly the aircraft can be loaded with each mission's specific payload. The first flight mission is a ferry flight with no payload installed. The aircraft's speed and maneuverability is tested by seeing how many laps around the flight course can be flown in four minutes. The second flight mission is a transport mission with an internal payload of a stack of three standard 2x6 wooden pine boards that are 10 inches long. The payload weighed a total of five pounds. It is a measure of how quickly three laps can be completed. The final flight mission is a drop mission. The payload is a team-selected number of 12 in. whiffle balls that are carried externally on the aircraft. It is a measure of how many laps can be completed successfully, where a successful lap is a complete lap around the flight course where only a single whiffle ball is dropped within the drop zone. The aircraft needed to be able to complete all four missions. Additionally, there were several other competition requirements, such that the aircraft must take off unassisted (using only the on-board propulsion system), needed to

land successfully (with no significant damage to the aircraft and without bouncing off of the runway), and could not be a rotary wing or lighter-than-air aircraft. There were also other safety requirements regarding the power and propulsion system.

The scoring of each mission and other competition requirements dictated the design choices for the aircraft. By analyzing the scoring equations, it was determined that the factors with the largest impact on the score were the empty weight of the aircraft as well as the complexity of the aircraft (the number of servos used). Thus, the team decided that a lightweight and simple aircraft needed to be designed. The mission requirements also dictated the design choices. Because the second flight mission's payload needed to be carried internally, the aircraft's fuselage needed to be large enough to hold it. However, the analysis of the scoring equations determined that the score of the final flight mission was weighted heaviest. Therefore, the team decided to design the aircraft in such a way to maximize this score. Much of the design time was focused on creating a successful dropping mechanism, and to maximize the aircraft's flight time in order to fly a large number of laps.

Conceptual Design

2.1 Mission Requirements

The 2014-2015 Design/Build/Fly “Remote Sensor Delivery and Drop System” is composed of four missions in total: one ground mission and three flight missions. Each mission has a different goal and different scoring parameters.

2.1.1 Mission and Scoring Summary

The overall competition is scored as shown in Equation 2.1. The score is dependent on the written report score (WRS), the total mission score (TMS) and the rated aircraft cost (RAC). The total mission score is the product of the ground score (GS) and the sum of the flight mission scores (M_i). This is shown in Equation 2.2. The rated aircraft cost is a measure of the complexity of the aircraft. It is dependent on the empty weight (EW) of the aircraft and the number of servos used in the aircraft (N_{servo}), as shown in Equation 2.3. The empty weight of the aircraft is measured after each scoring flight, and the maximum weight of the three is used. For each of these measurements, payload mounting or fairing provisions are included. In this competition, a servo is any mechanical or electronic device that is used to control the aircraft or the payload release mechanism.

$$Score = \frac{WRS * TMS}{RAC} \quad (2.1)$$

$$TMS = GS(M_1 + M_2 + M_3) \quad (2.2)$$

$$RAC = EW * N_{servo} \quad (2.3)$$

2.1.2 Flight Course

The general flight course is shown in Figure 2.1. This course is used in each flight mission. Each lap starts at the starting line. The aircraft must complete a rolling take-off within 60 feet of the starting line before climbing to an altitude that safely clears the terrain but also remains close enough to maintain unaided visual contact. After traveling 500 feet upwind of the starting line, a 180 degree turn must be completed, and the aircraft must be straight and level before starting the turn. The downwind leg is 1000 feet long. A 360 degree turn away from the course must be completed during this leg. Then, another 180 degree turn must be completed, with the aircraft straight and level before initiating the turn. After traveling 500 feet upwind, the aircraft must complete a safe landing on the paved portion of the runway. During landing, the aircraft may roll off the pavement, but may not bounce off. A flight will not be scored if the aircraft obtains significant damage during landing. This will be determined by the Flight Line Judge.

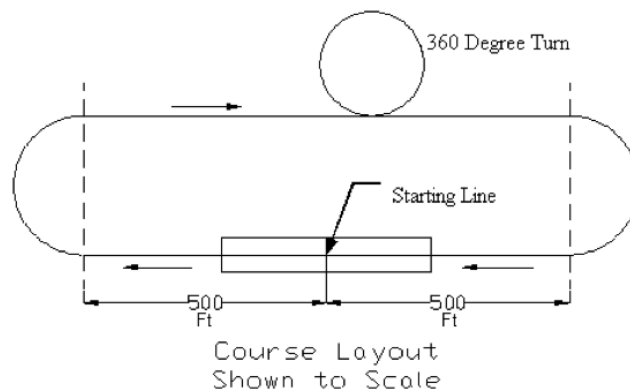


Figure 2.1: Flight Course

2.1.3 Ground Mission–Payload Loading Time

The ground mission is a measure of how quickly the different payloads can be loaded and unloaded. At the start of the mission, the aircraft is empty with all hatches or doors closed. When timing begins, the payload for Flight Mission 2 is loaded by the ground crew and the aircraft is closed as if for secure flight. The ground crew must then leave the loading area and timing is paused as the judge verifies that the payload is securely loaded. Timing is then restarted as the ground crew removes the Flight Mission 2 payload and inserts the Flight Mission 3 payload with the number of balls declared during the tech inspection. The ground crew must leave the loading area and timing is stopped. The judge will again verify that the payload is secured. The mission must be completed within five minutes.

The ground mission is scored relative to the fastest loading time in the entire competition, as shown in Equation 2.4. Therefore, the highest possible score for this mission is 1. A ground score of 0.2 is used for intermediate calculations if the mission has not been completed.

$$GS = \frac{\textit{FastestLoadingTime}}{\textit{LoadingTime}} \quad (2.4)$$

2.1.4 Flight Mission 1–Ferry Flight

Flight Mission 1 is a ferry flight with no payload installed based on how many laps are flown. The aircraft must take off within 60 feet. Once the throttle is engaged for the first take-off attempt, time is started. The aircraft must then complete as many laps as possible within a four minute flight time. A lap is considered complete once it passes over the starting line. After the flight time, the aircraft must complete a successful landing. If the aircraft is in the middle of a lap when the flight time expires, that lap will not be counted.

Flight Mission 1 is scored relative to the maximum number of laps flown by an aircraft in the competition, as shown in Equation 2.5. Therefore, the highest possible score for this mission is 2.

$$M_1 = 2\left(\frac{N_{laps}}{N_{maxlaps}}\right) \quad (2.5)$$

2.1.5 Flight Mission 2–Sensor Package Transport

Flight Mission 2 is a timed mission. The payload for this mission is one stack of three standard 2x6 wooden pine boards that are 10 inches long, as shown in Figure 2.2. The three boards are fastened together to form a block that is 4.5 inches by 5.5 inches by 10 inches and weighs about 5 pounds. The block has a dimension tolerance of $\pm 1/8$ inch in all directions. This payload is provided at the competition. The payload must be secured internally to the aircraft, where internal is defined as completely enclosed by aircraft structure or skin and is not exposed to any freestream air.

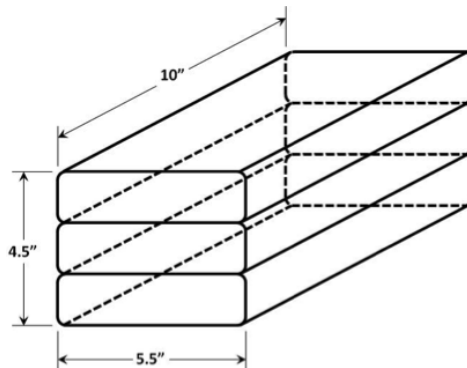


Figure 2.2: Flight Mission 2 Payload

Once the payload is loaded, the aircraft must take off within 60 feet. The aircraft must then complete three laps as quickly as possible. Time, measured in seconds, starts when the throttle is advanced for the first take-off attempt. Time ends when the aircraft passes over the finish line after completing the last lap. The aircraft must then land successfully in order to receive a score.

Flight Mission 2 is scored relative to the fastest time of an aircraft in the competition, as shown in Equation 2.6. Therefore, the highest possible score for this mission is 4.

$$M_2 = 4\left(\frac{T_{fastest}}{T_{flown}}\right) \quad (2.6)$$

2.1.6 Flight Mission 3–Sensor Drop

Flight Mission 3 is based on how many laps are flown and is not timed. The payload for this mission is a team-selected number of Champro 12 inch circumference whiffle balls as shown in Figure 2.3. Each ball weighs about 2.4 ounces. The balls are provided at the competition. The payload and all supporting equipment, including payload restraints and releasing mechanisms, must be secured externally. External is defined as exposed to freestream air when viewed from at least three sides.



Figure 2.3: Flight Mission 3 Payload

Once the payload is secured, the aircraft must take off within 60 ft. The aircraft will then fly laps around the flight course. On each lap, the aircraft must remotely drop one ball within the drop zone. The drop zone is defined as the 1000 foot upwind leg on the runway opposite the spectators, as shown in Figure 2.4. In order for the lap to be counted, only a single ball must be dropped within the drop zone. If multiple balls are dropped, that lap will not be counted. Additionally, no other part of the aircraft may be dropped with the ball, including any part of the payload mounting system. Finally, the aircraft must land successfully in order to receive a score.

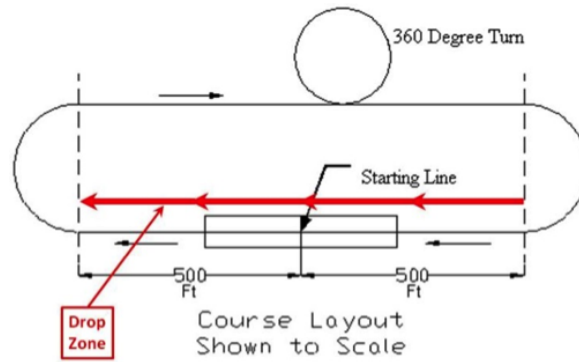


Figure 2.4: Flight Mission 3 Drop Zone

Flight Mission 3 is scored relative to the maximum number of laps flown by an aircraft in the competition, as shown in Equation 2.7. Therefore, the maximum possible score for this mission is 6.

$$M_3 = 6 \left(\frac{N_{laps}}{N_{maxlaps}} \right) \quad (2.7)$$

2.2 Mission to Design Requirements

2.2.1 Sensitivity Analysis

In order to determine which design aspects should be prioritized, a scoring sensitivity analysis was completed using the previously explained scoring equations and summarized in Equation 2.8 and Equation 2.9 below. This analysis did not include the score of the written report. The ground mission score was also assumed to be equal to 1, as there was no easy way for the team to estimate how other teams would perform in this mission. Finally, the number of servos was not included in the sensitivity analysis, though the general sensitivity is qualitatively comparable to the sensitivity of the empty weight, as both appear in the bottom of the fraction for the total score.

$$SCORE = \frac{GS(M_1 + M_2 + M_3)}{RAC} \quad (2.8)$$

$$SCORE = \frac{2\left(\frac{N_{laps}}{N_{maxlaps}}\right) + 4\left(\frac{T_{fastest}}{T_{flown}}\right) + 6\left(\frac{N_{laps}}{N_{maxlaps}}\right)}{EW * N_{servo}} \quad (2.9)$$

For this analysis, a set of baseline performance parameters were assumed based on research performed on previous competition performance as well as initial sizing estimates for the aircraft. This baseline can be seen in Table 2.1.

Table 2.1: Baseline Parameters used in scoring sensitivity analysis

Score Parameter	Top Performance	Baseline Assumption
Flight Mission 1	7 laps	4 laps
Flight Mission 2	150 seconds	207 seconds
Flight Mission 3	7 laps	4 laps
Empty Weight		6 lbs.

These values were then used in the scoring equation to calculate a baseline score of 1.867. Then, each parameter was increased and decreased by two percent of the baseline one at a time, up to an increase and a decrease of fifty percent. A new score was calculated, keeping the other parameters the same. The percent change in the score by changing a single parameter was then calculated and graphed versus the percent change in the parameter. This process was repeated for each score parameter shown in Table 2.1. The resulting scoring sensitivity graph can be seen in Figure 2.5, where N_{Laps1} is the number of laps flown in the first flight mission, T is the time that flight mission two was completed in, N_{laps3} is the number of laps flown in the third flight mission, and EW is the empty weight of the aircraft.

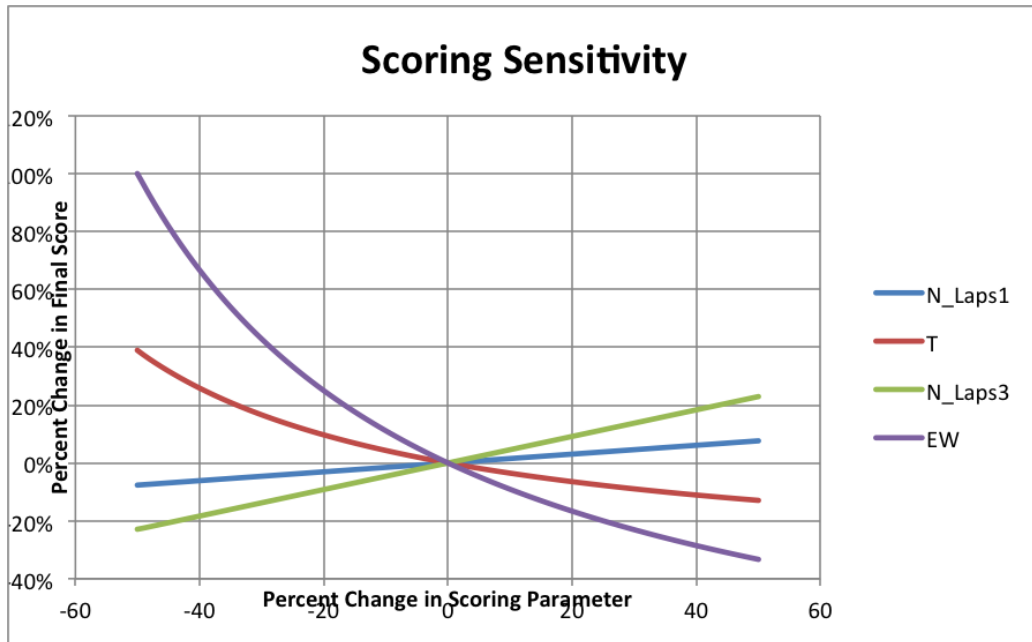


Figure 2.5: Scoring Sensitivity Analysis

A parameter that affects the final score more will produce a greater percent change in the final score in the same percent change of the parameter. Therefore, the sensitivity of each parameter can be qualitatively judged based on the slope of the curve. From Figure 2.5, it was clear to the team that the empty weight of the aircraft is the most important scoring parameter. This also could be seen in the scoring equations, as the total mission score is divided by the empty weight. The number of servos used by the team would have a similar sensitivity, as it also appears in the denominator of the scoring equation. The next most sensitive parameters are the number of laps flown in the third flight mission and the time taken to complete the second flight mission.

2.2.2 Design Constraints

The competition has several general requirements for the aircraft. First, it may not have a rotary wing or lighter-than-air configuration. No components or structure may be dropped from the aircraft during flight (except the flight mission three payload). The energy required for take-off must come from on-board propulsion system batteries (no form of

externally assisted take-off is allowed), and the aircraft must take off within 60 feet. Motors, propellers, blades, propeller hubs, and pitch mechanisms must be commercially available, though the propeller diameter may be modified and the blades may be painted to balance them. Unlike in previous years, there is no limit on the fuse rating for the motor, though it is up to the team to properly size the fuse. Batteries must be commercially available NiCad or NiMH, and the electrical contact points of battery packs must be protected (clear shrink wrap preferred). Battery disconnects must be fully insulated as well. The maximum weight of the battery pack(s) for propulsion is two pounds. Radio equipment and servos must use a separate battery pack. The aircraft take-off gross weight with payload must be below 55 pounds.

2.2.3 Design Requirements

Taking into account the scoring equations, scoring parameters, sensitivity analysis, and design constraints, some general design requirements could be determined. From the sensitivity analysis, a low empty weight has the largest impact on the final score, followed closely by the number of laps successfully completed in the third flight mission. To maximize the third flight mission score (the number of laps flown), it was desirable to maximize the amount of time the aircraft is in the air (loiter time). However, the weight of the battery pack is limited, therefore limiting the amount of power available to the propulsion system. Consequently, this implies that a light aircraft would be desirable to maximize the loiter time. To supplement this, a wing with a large coefficient of lift would be desirable in order to fly more laps in the third flight mission. Though increasing the number of laps flown in the third flight mission will subsequently add more weight to the aircraft in the form of increased payload and increased payload dropping mechanism and supporting structure, it was determined that this weight increase would be minimal with respect to the total aircraft weight.

The next most important score parameter is the time taken to complete the second flight

mission. This would imply that an aircraft with a higher speed would be desirable. This would also increase the number of laps that could be flown in the first flight mission. In order to meet this requirement with the limited power available for propulsion, an aircraft design with a low drag would be desirable. This low-drag design would impact fuselage design as well as the dropping mechanism and supporting structure for the payload in the third flight mission, as the payload must be loaded externally (exposed to freestream air).

One design requirement that was not taken into consideration in the sensitivity analysis is ease of loading the flight mission two and three payloads. This is quantified in the score for the ground mission. In order to minimize the time taken for this mission, the payloads must be easily accessible, and preferably able to be loaded and unloaded at the same time. It is important to minimize this time, as the ground score multiplies the sum of the flight mission scores. Another design requirement that was not taken into consideration in the sensitivity analysis is the complexity of the aircraft must be taken into consideration. This is quantified by the number of servos used in the aircraft. To maximize the final score, the number of servos used should be minimized. While the aircraft will need a certain number of servos to fly in order to operate the control surfaces, the dropping mechanism for the third flight mission should use as few servos as possible.

2.2.4 Battery Selection

After selecting an appropriate motor for the aircraft, a battery system to power it was chosen. Competition rules place a 2 lb. limit on the propulsion system batteries. Also, battery type is restricted to Nickel-Cadmium (NiCad) and Nickel-Metal Hydride (NiMH). After comparing the two types of batteries, NiMH was shown to be the better option. Nickel Metal Hydride batteries have a much longer lifespan than NiCad batteries, increasing loiter time for mission three. This quality, in addition to negligible memory effects far outweighed the slow charging rate of NiMH batteries. Furthermore, the ability to have multiple sets of batteries to switch between missions allows us to work around this problem.

2.3 Solutions Considered, Selection Process, Results

Once the mission requirements were translated into design parameters and restraints, a basic aircraft design could be created and considered. Because there are many solutions to solve the problems presented by the missions, the team determined a few parameters to use to judge each option. These parameters– or Figures of Merit –are listed below.

- **Weight**– This parameter is applicable in nearly all design decisions. From the sensitivity analysis, this parameter is the most important aspect of the aircraft in order to maximize the final score.
- **Payload Compatibility**– Three of the four missions (two flight missions and the ground mission) requires a payload in some way. For Flight Mission 2, the aircraft must ferry a specified payload. Therefore, the aircraft must be able to hold this payload. For Flight Mission 3, the aircraft must be able to hold a team-selected number of balls. This number of balls corresponds to the maximum possible score for this mission. In order to maximize the score, the largest number of balls without being detrimental to weight or any other parameters should be held. Finally, the payloads need to be held in an easily accessible fashion so that they may be loaded and unloaded quickly. This will minimize the time taken for the ground mission.
- **Lift**– In order to be able to successfully take-off, the aircraft must have high amounts of lift. A high lift will also allow the aircraft to loiter for longer, using less power. This is particularly important for Flight Mission 3.
- **Drag**– Flight Mission 2 is a measure of how quickly the aircraft can complete a specified number of laps. Flight Mission 1 is also an indirect measure of speed. In order to increase the final score, the aircraft should be speedy. In order to increase the speed, the drag created by the aircraft needed to be minimized.
- **Stability/Control**– In order to complete each mission successfully, the aircraft needed to be stable and controllable. This is particularly important during take-off and landing, as any aircraft that sustains significant damage during landing will not receive a score for that mission.
- **Manufacturability/Cost**– This parameter needed to always be considered. The aircraft design needed to be relatively easy to manufacture as limited by the team's

manufacturing experience. The design also needed to be fairly affordable, as the team had a strict budget

2.3.1 General Configuration

Several different options for the general shape and configuration of the aircraft: Conventional, Flying Wing, and Biplane. These were compared using the group's determined figures of merit on a scale of 1 to 3, where 3 is the best/most desirable rank in that category, as shown in Figure 2.6. Note that two configurations may have the same rank.

Figure of Merit	Weight	Conventional	Flying Wing	Biplane
Aircraft Weight	0.4	2	2	1
Payload Compatibility	0.2	2	1	2
Lift	0.1	1	3	2
Drag	0.1	2	2	2
Stability/Control	0.1	3	1	2
Manufacturability/Cost	0.1	3	1	2
Total	1	2.1	1.7	1.6

Figure 2.6: General Configuration

As seen in Figure 2.6, the Conventional configuration scored the highest. While the flying wing provides more lift, allowing for an aircraft with higher speed, the configuration also doesn't allow for much internal storage room because of the lack of distinct fuselage. Therefore, the aircraft would need to be much larger in order to accommodate the Flight Mission 2 payload. This would also increase the aircraft weight and manufacturability. The team was also generally unfamiliar with the manufacturing and handling of a flying wing aircraft. Therefore, a conventional configuration was selected due to its good weight, payload compatibility, stability, and manufacturability.

2.3.2 Wing Configuration

The next design choice that was considered was the wing design and configuration. It was decided upon early to use a simple rectangular wing to simplify construction and design of the wing. Two different wing placement configurations were considered: high wing and low wing. A high wing would be more stable, with much of the aircraft weight falling below the wings. However, extra structure would need to be added to the fuselage to support the Flight Mission 2 payload as well as the landing gear (it could not easily be attached to a wing box of any sort). A low wing would allow some of the wing structure to support the Flight Mission 2 payload and landing gear, but the aircraft would be more unstable. Ultimately, the extra weight added by adding necessary structure when using a high wing configuration was determined to be insignificant and a high wing configuration was chosen. This would also allow the wings to be easily removed for construction, repair, and to access the inside of the fuselage.

2.3.3 Motor Configuration

The next design choice that was considered was the motor configuration. This choice could have a large impact on the weight and balance of the aircraft, as well as the effectiveness of the propellers. Three options were considered: Pusher, Tractor, and Wing-Mounted. A Pusher configuration features the motor and propeller aft of the aircraft. A Tractor configuration features the motor and propeller in the nose of the aircraft. Twin Wing-Mounted motors would have two smaller motors and propellers mounted on the leading edge of the wings. The following figures of merit were considered, as shown in Figure 2.7.

Figure of Merit	Weight	Pusher	Tractor	Twin Wing-Mounted
Aircraft Weight	0.4	3	3	1
Efficiency	0.2	1	3	1
Landing Gear Interference	0.2	1	2	2
Manufacturability/Cost	0.2	2	2	1
Total	1	2	2.6	1.2

Figure 2.7: Motor Configuration

Ultimately, the Tractor configuration was chosen. Two wing-mounted motors would not add any efficiency, and would require extra structural support in the wings. It would also add to the cost. A Pusher configuration would also add weight and complexity to the aircraft, as the weight of the battery, motor, and propeller on the aft of the aircraft would need to be balanced with extra weight at the nose of the aircraft. The Tractor configuration is relatively simple and familiar to the group, which are several reasons why it was chosen.

2.3.4 Landing Gear Configuration

The landing gear configuration was an important decision for several reasons. The landing gear needs to be able to support the weight of the aircraft with all payloads loaded. It must also help meet the take-off requirement. Finally, it must be able to support the aircraft upon landing. Landing gear failure at landing would invalidate the score of that particular flight mission. Three configurations were considered: Tricycle, Bicycle, and Tail Dragger. A tricycle configuration features two main wheels slightly aft of the center of gravity and a third wheel on the nose of the aircraft. A bicycle configuration features two wheels along the centerline of the aircraft and a small wheel near the tip of each wing. A tail dragger configuration features two main wheels slightly forward of the center of gravity, with a third tail near the tail of the aircraft. The options were weight using several of the team's figures of merit, as shown in Figure 2.8.

Figure of Merit	Weight	Tricycle	Bicycle	Tail Dragger
Aircraft Weight	0.4	2	2	2
Drag	0.3	2	1	3
Handling	0.15	2	1	2
Stability	0.15	2	1	2
Total	1	2	1.4	2.3

Figure 2.8: Landing Gear Configuration

Ultimately, the tail dragger configuration was chosen. The tricycle configuration was nearly chosen, but it was decided that the front wheel would be located too close to the nose-mounted propeller, decreasing its effectiveness and increasing overall drag of the aircraft. The tail dragger would provide good stability and drag characteristics, and would help the aircraft reach the desired angle of attack for take-off.

2.3.5 Tail Configuration

The tail configuration is an important design choice as it features several of the control surfaces of the aircraft which contribute to its control, handling, and stability. Three configurations were considered: Conventional, T-Tail, and V-Tail. A conventional tail consists of a vertical stabilizer on top of a horizontal stabilizer. The horizontal stabilizer's elevator helps to control pitch, while the vertical stabilizer's rudder helps to control yaw. A T-Tail consists of a horizontal stabilizer on top of a vertical stabilizer. A V-Tail features two identical stabilizers offset from the horizontal at a certain angle, with a coupled rudder-elevator. The choices were judged using several figures of merit, as shown in Table 2.9.

Figure of Merit	Weight	Conventional	T-Tail	V-Tail
Aircraft Weight	0.5	2	1	2
Stability and Control	0.3	3	2	1
Drag	0.2	2	3	3
Total	1	2.3	1.7	1.9

Figure 2.9: Tail Configuration

The conventional configuration was chosen due to its overall good weight, stability, control, and drag characteristics. A T-Tail would require extra structure throughout the vertical stabilizer in order to support the horizontal stabilizer and the loads it creates. However, it would increase the effectiveness of the horizontal stabilizer because it would lift it out of the way of the wake of the wings. A V-Tail would allow for a smaller tail due to the angled stabilizers, but this would increase the difficulty of controlling the aircraft due to the yaw and pitch control being coupled. Overall, the conventional configuration was chosen due to familiarity, ease of manufacturing, and good stability and control characteristics.

Preliminary Design

3.1 Design Methodology

3.1.1 Wings

- **Wing Area**–The team decided to focus on a large wing area in order to generate adequate lift for carrying the various payloads during the competition. This led to a total wing area of 11.67 square ft. with a 10 ft. wingspan and 14 in. chord.
- **Aspect Ratio**– The wing was designed with a fairly high aspect ratio of approximately 8.5 in order to make for more efficient flight while shortening the take-off distance to fulfill the 60 ft. requirement.
- **Airfoil**– The team designed a custom, high-camber, airfoil to yet again increase lift and lift-to-drag performance.
- **Dihedral**– The dihedral was designed to increase roll stability as well as induce a roll when the rudder is activated. This would allow for the aircraft to fly controlled turns without the use of ailerons and reduce the required number of servos, thereby increasing the total score.
- **Structure**– The wing was built up of carbon fiber spars, balsa ribs, a balsa and carbon fiber laid D-cell, and a balsa and bass wood dihedral box. These components were crucial to the design when considering the large wingspan. The team focused on making the wing strong and rigid to withstand wing loading in-flight and on landing while keeping them as light as possible.

3.1.2 Fuselage

- **Bulkheads**– The main shape of the fuselage was formed by a series of rectangular and hexagonal bulkheads made of balsa plywood.

- **Stringers**– The fuselage also contained stringers made of 1/8” carbon fiber tubes going along the outside of the bulkheads.
- **Truss**– To create a more rigid structure, several 1/8” balsa strips were formed into a truss system in the rear portion of the fuselage.

3.1.3 Empennage

- **Control Surfaces**– The team decided to reduce the number of servos by removing the ailerons and use a full-flying tail with dihedral. Therefore, the tail structure and surfaces needed to be sufficient for controlling the entire aircraft.
- **Horizontal Tail Structure**– The design consisted mainly of a small piece of tubular carbon fiber spar to attach to the control arm and then distributed the stresses through thin strips of balsa, balsa ribs, and a balsa D-cell.
- **Vertical Tail Structure**– Contrary to the horizontal tail, this included a carbon fiber spar throughout the entire span. It also included a balsa D-cell in front and thin balsa strips towards the back. The vertical tail also included a slight taper.

3.1.4 Propulsion

Motor, Electronic Speed Controller, Battery, and Propeller– In contrast to many standard R/C aircraft, this design calls for a much larger required payload and overall aircraft weight. In accordance with the AIAA’s regulation for a 2 lb. maximum battery weight, the battery was selected in order to maximize power within the limitation. Additionally, the motor and battery were selected in order to maximize thrust while the brushless motor maintained high efficiency.

3.2 Drop Mechanism

The payload mission offered the biggest challenge of the entire build. In order to optimize our score, we needed to maximize our payload while minimizing our servo count. We began by establishing five design goals:

1. Limit the servo count to 1 servo
2. Design it as reliably as possible
3. Design it to have veritable payload
4. Design it to be modular
5. Design it as simple as possible

The initial designs were focused around a tube that would contain the balls, and a release mechanism at one end of the tube that would allow one ball to leave the tube per actuation. This idea was designed, and a prototype was built in the first few weeks as a proof of concept. A change of rules at the end of October required that all of the balls be mounted externally to the aircraft. This led to the dismissal of the original design, and a completely new set of ideas that would not require the balls to be contained in a tube.

The next breakthrough in the design of the drop mechanism was creating and using a ratchet to control the drop of each ball from the aircraft. In order to meet the requirements of dropping one ball per lap, and keeping the number of servos to a minimum, using a ratchet was suggested as it can accomplish the task with a single servo. The ratchet takes the motion from the servo and uses it to push a gear one step. The servo returning to its original state reloads the ratchet arm, making it ready to turn the gear again on the next actuation of the servo. Once the team decided that the goal was to drop a maximum of 7 balls, a ratchet with 8 steps was designed, allowing one step for each ball drop and one for the initial loading and flight.

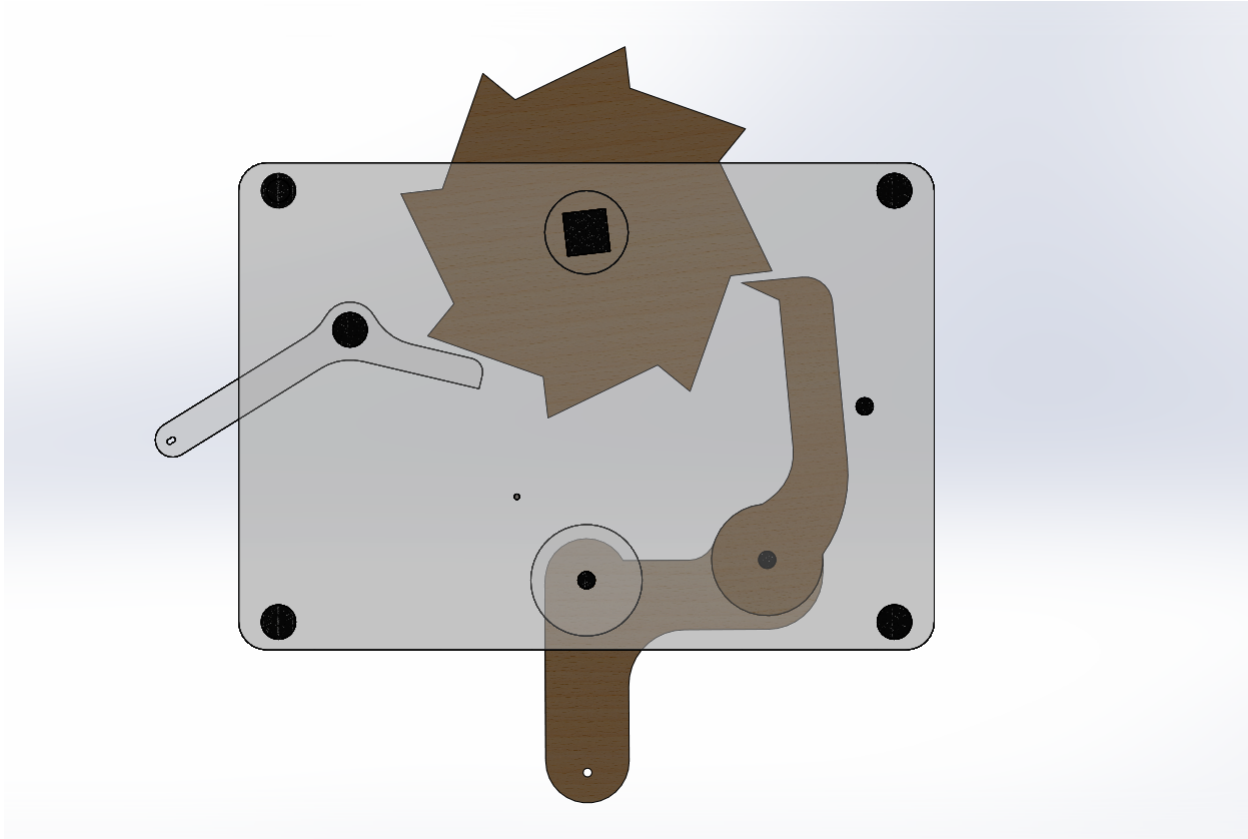


Figure 3.1: Ratchet Mechanism

Once the ratchet was developed, different mechanisms were designed that held the balls in place until they were released. Some ideas involved a cage made up of 1/8 inch carbon fiber tubes rotating with each servo motion, while others were sliding wires or rods that moved a certain distance with each actuation. A camshaft was eventually selected to control the release of one ball at a time. The camshaft attached to the gear in the ratchet, and also moved 1/8 of its rotation with each actuation, causing one cam at a time to point directly downwards and release a ball.

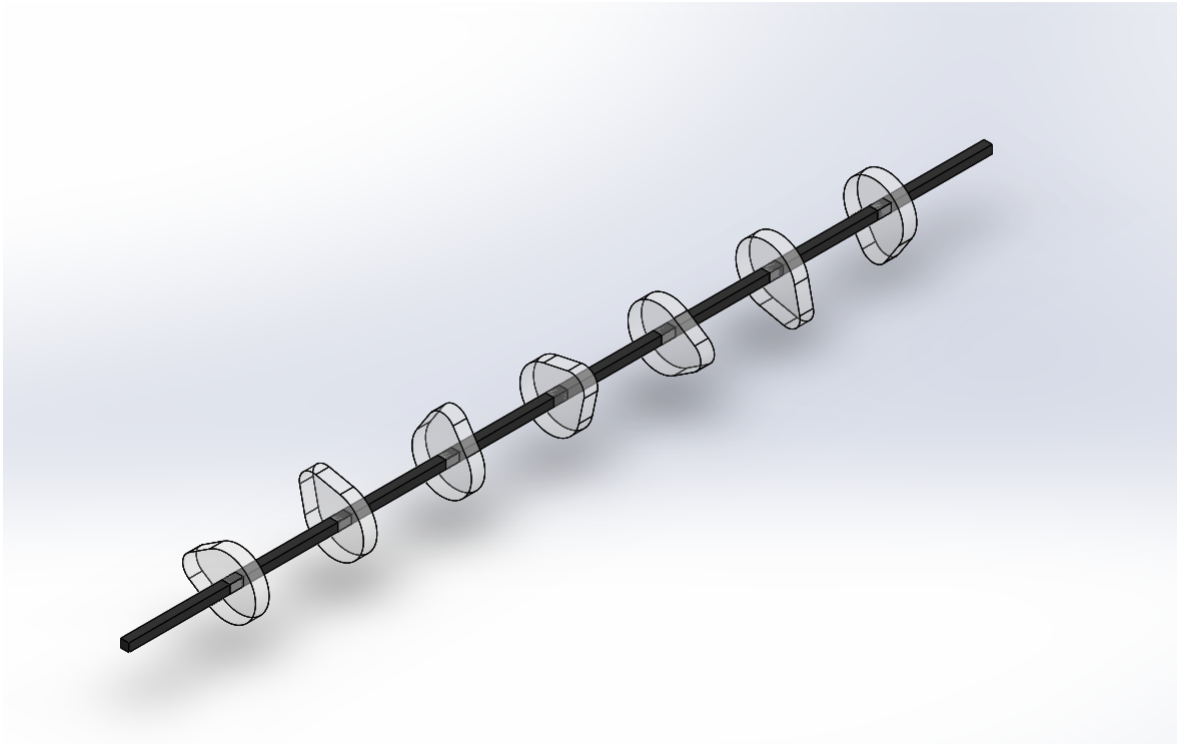


Figure 3.2: Drop Mechanism Camshaft

With the development of the ratchet and cam ideas, multiple release mechanisms were designed and tested. Many faced problems with jamming, loading difficulty, or being too difficult to manufacture. The final design will be discussed in detail in section 4.3.5.

3.3 Sizing and Trade Studies

The aircraft design process includes several trade studies that need to be done in order to find optimal design characteristics. These trade studies focus on achieving a certain maximum performance while balancing two or more potential designs. This project accomplished these trade studies on several components such as airfoils (Section 3.5.1), tail sizing (Section 4.1), and control surfaces (Section 3.5.3). Those trade studies are discussed in detail within their respective sections of the report.

3.4 Mission Model

Considering the various missions the aircraft would complete, the team considered mission profiles for each part of the competition. This was utilized for optimizing results and increasing the maximum achievable score. Each flight mission shared a few of the same mission legs, namely take-off, climb, cruise, turn, and descend. However, some of the missions required specific mission planning.

Mission 1 was an empty flight designed for speed. Mission 2 also was designed for speed but included a wooden payload. Finally, flight Mission 3 was focused on a long battery lifespan and good range specifications. With these details in mind, the team came up with mission profiles as described below.

Flight Missions 1 and 2:

- Take off within 60 ft., increase altitude to about 75 ft.
- Level off, maintain max speed
- Slow down to execute tight turns as necessary
- Decelerate and descend in landing approach, execute landing

Flight Mission 3:

- Take off within 60 ft., increase altitude to about 75 ft.
- Reduce power on straights to conserve power
- Re-engage motor for turns, maintain altitude
- Drop ball when over target area, repeat once each lap until payload used completely
- Decelerate and descend in landing approach, execute landing

3.5 Aircraft Characteristics

3.5.1 Final Airfoil Selection Analysis

The primary goal in selecting the proper airfoil design was to optimize a standardized NACA airfoil by modifying it for relatively low speed and high lift. The most important factor to account for in the airfoil analysis was to account for take-off conditions speeds. In order to have an effective takeoff, the aircraft must be able to provide enough lift at low, stable speeds with increasing angle of attack from 0 degrees to our defined maximum angle of attack of 10 degrees (in order to reach a safe flight height before the first turn).

The most valuable tool throughout this analysis was XFLR5 [6], an airflow simulator that provides the polar graphs for Lift Coefficient vs. Drag Coefficient and Lift Coefficient vs. Angle of Attack. Based on our approximations, supported by previous DBF competitions the approximate cruise speed would be 45 mph. After conversing with our test pilot, a safe takeoff speed is slightly greater than half of the max cruise speed. Therefore, we took our takeoff speed to be 25 mph. In order to keep track of all relevant input data, an Excel analytical tool was developed for further use in calculating lift, after airfoil modeling was performed. Data such as chord length, aircraft, air density/viscosity, and wing surface area were all tabulated.

In order to provide an accurate Lift Coefficient (C_L), the proper Reynolds number and Mach number were input. Before XFLR5 [6] modeling could be completed, Reynold's number and Mach number were calculated using the following equations:

$$R_e = \frac{V * Chord}{\nu} \quad (3.1)$$

$$M = \frac{V}{c} \quad (3.2)$$

To calculate the Reynolds number, we chose a chord length of 14 in. in order to increase

surface area, without making an exceedingly thick airfoil. Thin airfoils are considered to be more effective at low speeds. Both values (302157 and 0.03592 respectively) were input to XFLR5 [6] before any airfoil selections were made. All airfoil tests were run for a range of angle of attack from -10 degrees to 20 degrees in order to model the lift in descent, as well as climb, and accurately observe the stall angle.

Based upon previous reviews throughout the R/C aircraft community found in forums [5], one of the best and most utilized airfoils is the NACA 4412. After the airfoil was designed in the program, plots for C_l vs. C_d and C_l vs. AoA were produced, as seen in Figure 3.3 below.

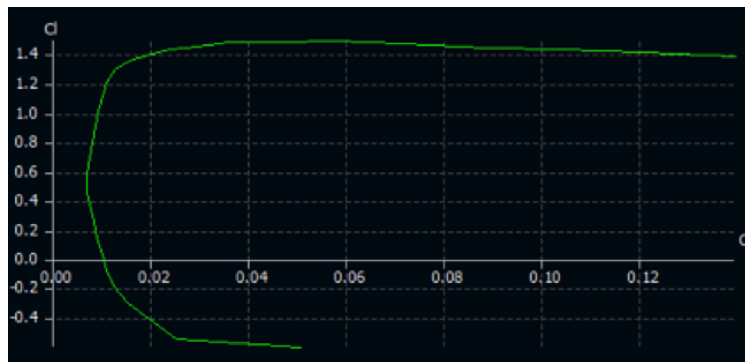


Figure 3.3: C_l v C_d of NACA 4412

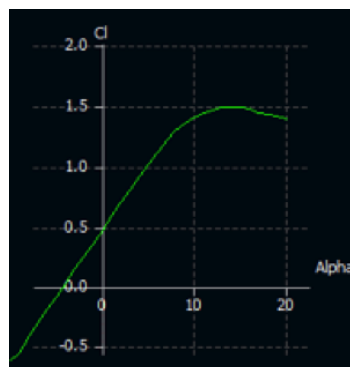


Figure 3.4: C_l v AoA for NACA 4412

As previously stated, the most important values from these models are the instances of takeoff at angle of attack equal to 0. Essentially, these models aim to demonstrate whether the aircraft will takeoff. The C_l at angle of attack (roughly 0.45) was then used to calculate

the lift from our predetermined variables (wing span = 10 ft. chord length = 14 in.). The equation for lift is shown below, and Figure 3.4 illustrates the The C_l versus angle of attack.

$$Lift = \frac{1}{2}\rho V^2 S \quad (3.3)$$

In the Excel analytical tool, a True-False statement was inserted to indicate whether the airfoil would provide enough lift to achieve stable flight. The NACA 4412 would not suffice. At the suggestion of one of the underclassmen on the aerodynamics and propulsion team, XFLR5 [6] analysis was performed for a variety of decreased thicknesses and increased camber. The results from these tests can be found in Figure 3.5 and Figure 3.6 below.

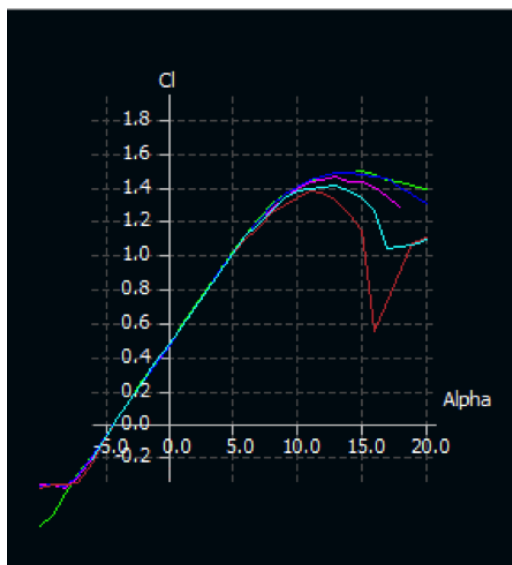


Figure 3.5: C_l v AoA for Decreased Airfoil Thickness

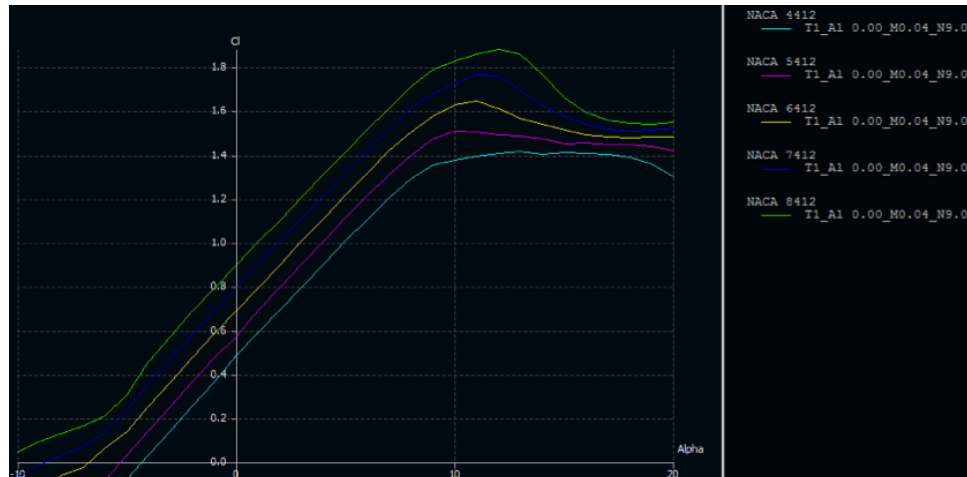


Figure 3.6: C_l v AoA for Increased Airfoil Camber

It is clear from the figures that decreasing the airfoil thickness yielded very little change, while increased camber at such low speeds doubled the Coefficient of Lift at a camber of 8% vs. the original of 4%. While testing above 8% camber were performed, they were deemed unusable due to the inability to properly apply the ultracoating material to the full-scale wing. The 8% camber was demonstrated to be the limit where ultracote could be properly applied and not peel off due to the induced tension.

Similar to the initial calculation, the lift from an 8% camber airfoil at an angle of attack of 0 degrees was calculated to be 86 Newtons (approximately 19 lbs.). This would allow for the aircraft to takeoff and ascend safely and in a stable manner as the coefficient of lift increases linearly as AoA until approximately 10 degrees. Additionally, after the 8% camber was successful in providing enough lift for the aircraft, the C_l vs. C_d graph was analyzed to ensure a smooth curve and high lift-to-drag ratio. The graph can be found below in Figure 3.7

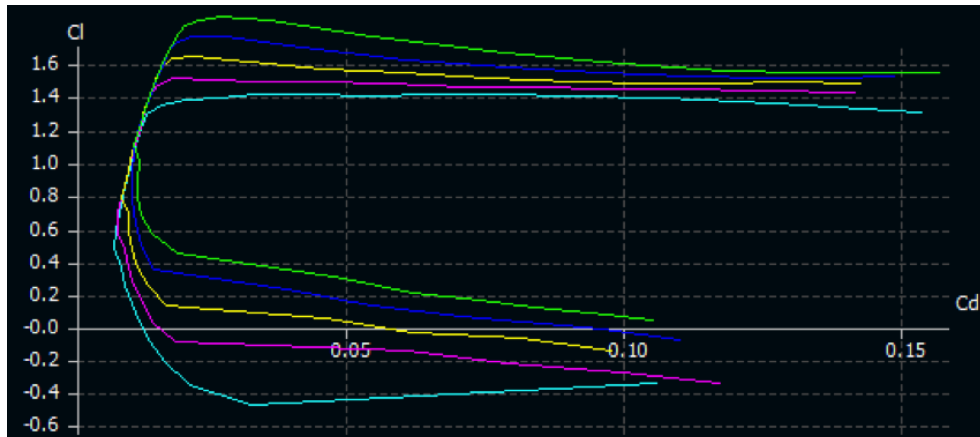


Figure 3.7: C_l v C_d for Varying Airfoil Camber, Teal-4%, Green-8%

It is visually clear that as camber percentage is increased, the lift-to-drag ratio improves drastically. After completing the airfoil analytical tool, it was evident that the 4% camber increase to the NACA 4412 was not only necessary, but vastly improved its ability to provide substantial lift.

3.5.2 Drag Estimate

In order to calculate the total drag of the aircraft, individual section's parasitic drag were calculated alongside the induced drag. Using the aircraft drag build-up method, the overall coefficient of drag was calculated. Due to the aircraft's particular specifications (rigid landing gear and fully-exposed Whiffle Balls), Raymer's *Aircraft Design* [4] was utilized to obtain proper values and equations. The equations used for induced drag can be found below. The value e is the Oswald Efficiency Factor which is taken to be 0.8. Additionally, the collective drag coefficients and their respective percentage to the overall can be found in the table and pie chart below.

$$C_{D_{ind}} = \frac{C_L^2}{\pi A R_{wing} e} \quad (3.4)$$

Aircraft Component	Coefficient of Drag
Wing	0.008616
H. Tail	0.006198
V. Tail	0.005704
Fuselage	0.003088
Landing Gear	0.043365
Wiffle Balls	0.03927
Induced Drag	0.037619
Total Drag	0.143861

Figure 3.8: Aircraft Component Coefficient of Drag

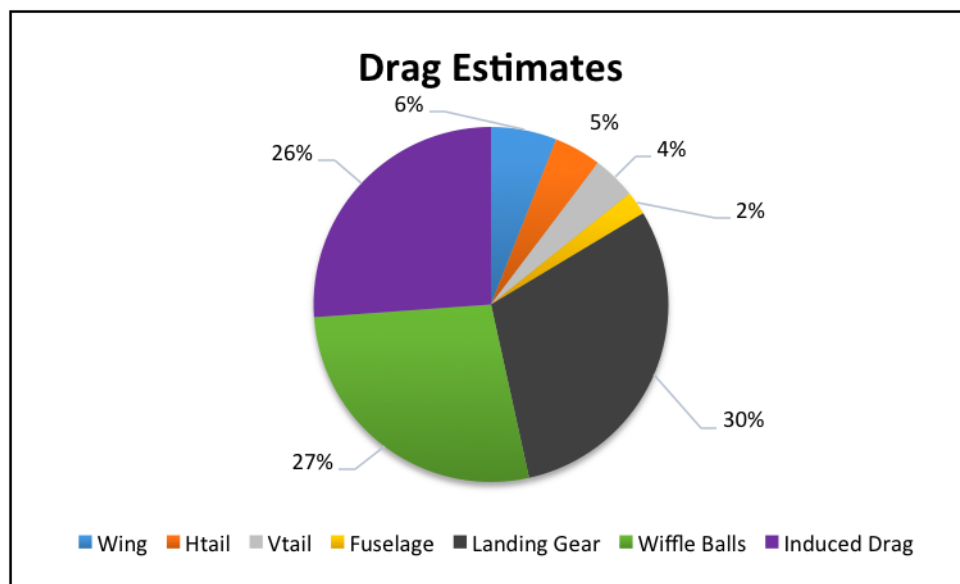


Figure 3.9: Aircraft Drag Buildup Percentages

3.5.3 Stability and Control

Aerodynamic Center

In order to determine the static margin of the aircraft, an aerodynamic center analysis was performed. This was done to ensure that the aerodynamic center of the entire aircraft was located behind the center of gravity, indicating aircraft stability. This analysis was performed using MATLAB [2] to easily adjust any aircraft values throughout the entire design process. Additionally, Napolitano's *Aircraft Dynamics* [3] was utilized for guidance and figure interpolation for aircraft specific values and constants.

The first step of the process was defining a list of aircraft specification inputs, including root wing span, mach number, aspect ratio, etc. It was particularly important to perform a build-up analysis of our main wing due to its three-section structure with induced dihedral on the outer wing sections. In addition to the major steps for calculating aerodynamic center values, various intermediate steps were performed to obtain required values. The most detailed of these steps was applying Munk's Theory to calculate the aerodynamic center shift of the fuselage. In order to complete this task, the aircraft fuselage was discretized into thirteen individual sections with defined length, distance from the wing, and width. Using SolidWorks sketches of the fuselage outline, all values were tabulated and used in the final calculation. A visual representation can be found below to better detail the process of discretization.

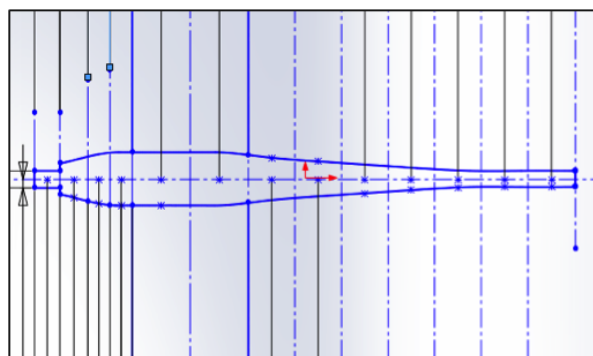


Figure 3.10: Munk's Diagram

After all intermediate steps and interpolations from Napolitano's [3] figures were completed, the aerodynamic center build-up method was complete. The following table provides the calculated values from the overall analysis, in the order that they were performed.

Aerodynamic Center	Value
Wing	0.2500
Horizontal Stabilizer	4.6505
Vertical Stabilizer	5.2943
Wing and Body	-0.0230
Aircraft	0.2902

Figure 3.11: Aerodynamic Center Calculations

After the final calculation was performed, the total aircraft aerodynamic center is 0.2902 (in reference to a percentage of the chord). In comparison to the center of gravity, the aerodynamic center lies behind it, indicating stability in flight.

Stability Analysis

In a similar fashion to the aerodynamic center calculations, Napolitano's *Aircraft Dynamics* [3] was utilized in calculating the aircraft stability derivatives. While the magnitude of the stability derivatives is valuable, the true value lies in its sign notation (positive or negative). After performing the analysis for the final design, all required parameters fell within the correct sign notation. A table of these values can be found below in Figure 3.12.

$C_{L,\alpha}$	$C_{L,\delta,E}$	$C_{L,q}$	$C_{m,\alpha}$	$C_{m,\delta,E}$	$C_{m,q}$
5.6078	0.5020	7.0440	-0.2191	-2.2085	-19.9911
$C_{Y,\beta}$	$C_{l,\beta}$	$C_{n,\beta}$	$C_{Y,\delta,A}$	$C_{l,\delta,A}$	$C_{n,\delta,A}$
-0.5486	-0.0615	0.2499	0.0000	0.0000	0.0000
$C_{Y,\delta,r}$	$C_{l,\delta,r}$	$C_{n,\delta,r}$	$C_{Y,p}$	$C_{L,p}$	$C_{n,p}$
0.2436	0.0000	-0.1095	-0.0607	-0.5039	-0.0298
$C_{Y,r}$	$C_{L,r}$	$C_{n,r}$			
0.4999	0.1169	-0.2403			

Figure 3.12: Stability Derivatives

Control Surface Sizing

In order to maximize the final competition score, the team decided to minimize the total number of servos in the aircraft. The control scheme is therefore slightly modified from the conventional rudder, elevator, and aileron configuration. This standard configuration would require three or four servos, but by steering entirely with the tail rudder and elevator, a two-servo control system is possible. Therefore, we implemented a dihedral angle in the main wing to help induce roll with a full-flying tail. The entire vertical stabilizer and the entire horizontal stabilizer of the tail function as the control surfaces, rotating about spars located on their aerodynamic centers.

To analyze the airfoil choices for the control surfaces, analysis software XFLR5 [6] was used. Several symmetric airfoils which usually exhibit desirable behavior at low Reynolds numbers were tested. This included the HT 14, NACA 0012, S9026, and a modified NACA 0012, with a maximum thickness of 11.1% located at 22% of the chord.

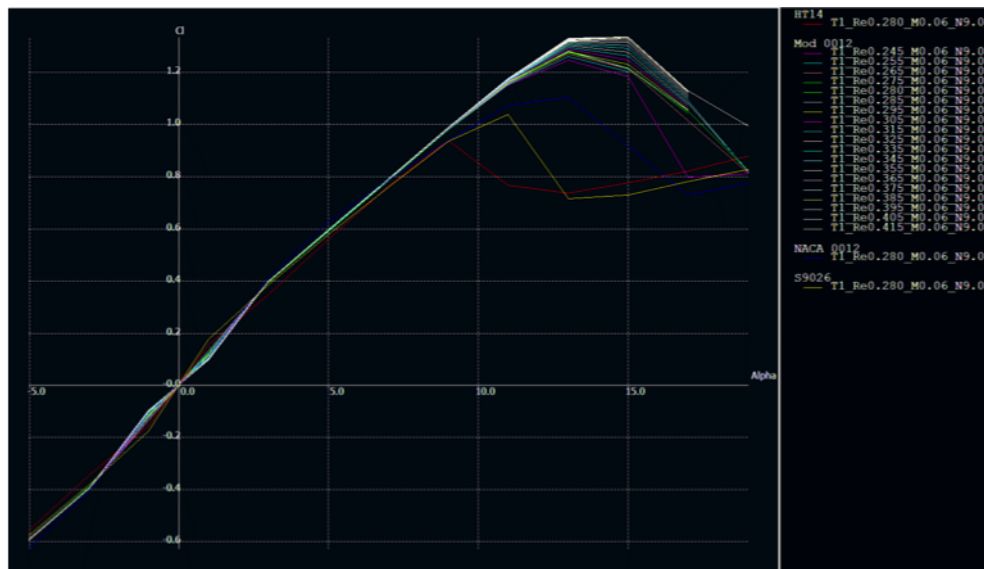


Figure 3.13: NACA 0012 tail airfoil analysis

The clear frontrunner of these analysis results was the modified NACA 0012, which was further analyzed for a range of Reynolds numbers to determine the optimum chord length. It was found that for the expected take-off velocity of 14 m/s, a chord length of roughly 10 inches would meet the needs of the control surfaces.

$$R_e = \frac{\rho VC}{\mu} = \frac{(1.2255)(14)(0.254)}{(1.846 * 10^{-5})} = 236071 \quad (3.5)$$

This Reynolds number will increase at cruise, as the velocity increases to 20 m/s, and the range of Reynolds numbers analyzed indicates that performance will improve at these speeds.

In order to determine the necessary span of the control surfaces, a mathematical model was used to determine the lift force necessary to execute a 1g turn at 20 m/s.

$$a = \frac{v^2}{r} \rightarrow r = \frac{(20 \frac{m}{s})^2}{9.8m/s^2} = 40.8m \quad (3.6)$$

$$L = ma = (5kg)(9.80 \frac{m}{s^2}) = 49N \quad (3.7)$$

$$L = C_L q S \rightarrow S = \frac{L}{C_L q} = \frac{49N}{(1.2)(0.5)(1.2255 \frac{kg}{m^3})(20 \frac{m}{s^2})} = 0.167m^2 \quad (3.8)$$

$$bc = S \rightarrow b = \frac{S}{c} = \frac{0.167m^2}{0.254m} = 0.656m = 25.8in \quad (3.9)$$

This indicates that a 1g turn could be executed at 20 m/s with a control surface of 0.167 m². Thus, the elevator was designed with a span of 28 inches and chord of 8 inches, while the tapered rudder was designed with an average chord of 8.8 inches and a span of 11.33 inches.

3.5.4 Structural Design

In order to maximize the overall score in the competition, it was necessary to reduce weight wherever possible. The initial designs for our internal support structures were focused on strength and durability, with some attention towards weight, but once early manufacturing and testing were conducted, designs were revised to focus on weight considerations. Ease of manufacture also became of concern as our resources in terms of time and money were not unlimited. However, it was always the primary goal to attain a deliverable with the desired performance characteristics.

Wing Structure

From the outset, it was the intention of the team to design a wing with a high aspect ratio similar to that of a glider to promote efficiency at low Reynolds numbers. A wingspan of 10 feet would be no small task to design durably while minimizing weight. A dihedral angle was also necessary to ensure the airframe would roll with a two-axis control system. In order to meet these concerns, tubular carbon fiber spars were chosen. Despite a high cost point, these spars would be light, extremely strong, and would remain rigid across the span. A typical built-up balsa spar would likely have had serious difficulty in matching these

properties.



Figure 3.14: Wing Structure

The planform of our wing is rectangular. It was concluded that there would be little gain from significant taper or twist at such low speeds. Swept wings were also ruled out for the same reason and for manufacturability. The same airfoil is used across the full span. This airfoil shape, the NACA 8412, was established with laser-cut 0.125 inch thick balsa ribs, spaced 3 inches apart. These ribs have lightening holes to reduce weight. A balsa and carbon fiber D-cell wraps from the quarter-chord of the lower surface to the quarter-chord of the upper surface, structurally strengthening the leading edge of the wing. The D-cell also promotes shear flow of the longitudinal forces caused by air flow against the leading edge. The front spar, centered at the quarter-chord, has an outer diameter of 0.752 inches. The rear spar, centered 5.625 inches from the front spar, has an outer diameter of 0.501 inches. There is also a 0.125 inch thick carbon fiber rod supporting the trailing edge of the wing. These components are effective in preventing torsion.

To establish a dihedral angle in the wing, it was broken into three sections. A four foot span is centered over the fuselage, and is removable for payload loading. There are two outer three foot sections which connect to the center section at an angle five degrees above the lateral axis of the wing. At these joints, a box made of basswood surrounds the front and rear spars of the center and outer wing sections, holding them in the desired dihedral angle. This also addressed another key design parameter, the overall modularity of the airframe.

By breaking the wing into shorter sections, transport and repairs will be simpler.

The wing sections are wrapped with ultracote. Scalloping effects are reduced by the relatively close rib spacing, resulting in a smooth upper and lower airfoil surface, and generating the most lift.

Fuselage Structure

The basic structure of the fuselage consists of bulkheads made from balsa ply of varying thicknesses, spaced by roughly 6 inches, and connected longitudinally by carbon fiber stringer tubes 0.125 inches in diameter. These stringers are somewhat flexible, allowing for a streamlined fuselage shape.

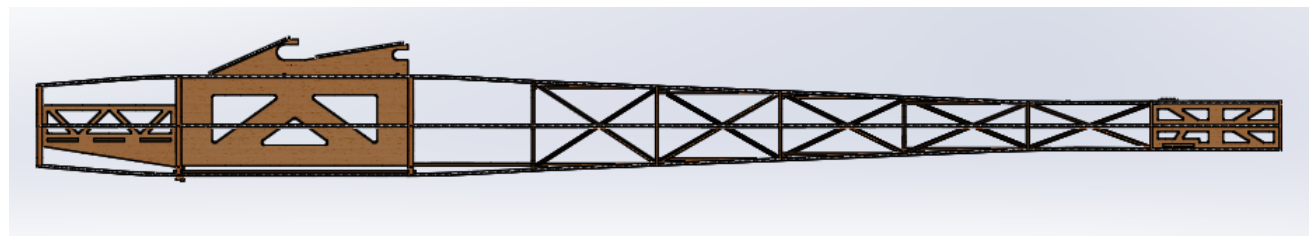


Figure 3.15: Fuselage Model

The motor will mount to the forward bulkhead, with the propulsion system battery located in the walled box just behind. The payload will rest between the second and third bulkheads, which are separated by 11.25 inches. This cargo compartment is also walled and has a floor for the payload to rest on. The payload will also be further secured with Velcro straps. The walls of the compartment also function as the mounting system for the main wing. Reinforced with Kevlar twine, 0.125 inch carbon fiber tubes, the hooks on these walls will support the lifting force of the wing. Elastic bands will also be implemented for further support. The dropping mechanism for the second payload will mount below the cargo compartment of the fuselage and also secure to the floor between the third and fourth bulkheads. The ninth and tenth bulkheads are walled to support the horizontal and vertical tails as well as the servos that operate them.

The space between the fourth and ninth bulkheads is essentially empty, but given the layout of the longitudinal stringers, is prone to twist. To compensate for this effect, balsa trussing was added in with the goal of reducing weight as much as possible. With the addition of this trussing, the twist across the length of the fuselage is minimal.



Figure 3.16: Fuselage Trussing

The overall fuselage length is 5.03 feet. The widest and tallest section is the cargo compartment, with a width of 0.53 feet and a height of 0.41 feet. The stringers are secured to the bulkhead with a combination of CA glue and Kevlar twine. Bulkheads, floors, and walls are complete with lightening holes where possible to further minimize weight.

3.6 Preliminary Mission Performance

After an aircraft design was chosen, an estimation of each mission score was obtained using values computed during the preliminary analysis. The individual missions were evaluated according to Figure 3.17, and a list of relevant performance parameters for each mission is detailed in Figure 3.18.

	Vehicle Parameter	Scoring Parameter
Mission 1	Speed	Number of Laps in 4 Minutes
Mission 2	Heavy Weight (5lb)	Time to Complete 3 Laps
Mission 3	Time Aloft, Payload Capacity	Payload Dropped

Figure 3.17: Mission Evaluation

Performance Parameter	Mission 1	Mission 2	Mission 3
$C_{L,max}$	1.8	1.8	1.8
$C_{L,cruise}$	0.9	0.9	0.9
$C_{D,0}$	0.1027	0.1046	0.1439
L/D_{max}	10.9283	10.9283	10.9283
L/D_{cruise}	7.6475	7.3359	5.4925
Rate of Climb	10.07 ft/s	6.42 ft/s	7.64 ft/s
W/S [lb/ft. ²]	0.626	1.055	0.676
Cruise Speed	45 mph	35 mph	30 mph
Gross Weight	7.845 lbs.	12.845 lbs.	8.423 lbs
N_{laps}	4	4	7
W_{cargo}	N/A	5 lbs.	0.577 lbs.
Predicted Mission Score	1.1429	2.2857	5.25

Figure 3.18: Mission Analysis

None of the individual mission scores are expected to be the best in the competition. However, due to the high carrying capacity of the aircraft and the low number of flight control servos, a relatively high final score is expected.

Detail Design

Building off of the preliminary design, the next step of the process involves detail design. This begins to factor in more specific design criteria due to physical limitations, not only mathematical models and computer programs. This phase of the project resulted in the final designs of each component— structural, geometrical, electrical, and aerodynamic.

4.1 Dimensions and Parameters

Wing		Fuselage	
Airfoil	NACA 8412	Length	5.04 ft (1.54 m)
Span	10 ft (3.05 m)	Width	0.53 ft (0.162 m)
MAC	14 in (0.356m)	Height	0.41 ft (0.124 m)
Wing Area	11.67 ft ² (1.08 m ²)		
Aspect Ratio	8.57		
Incidence Angle	0°		
SM	4.12%		

(a) Wing Dimensions

(b) Fuselage Dimensions

Figure 4.1: Wing and Fuselage Dimensions

Tail Surfaces		
	Horizontal	Vertical
Airfoil	NACA 0011 with maximum thickness at 22% of MAC	
Span	2.33 ft (0.711 m)	0.979 ft (0.298 m)
MAC	0.667 ft (0.203 m)	0.723 ft (0.220 m)
Wing Area	1.55 ft ² (0.144 m ²)	0.708 ft ² (0.066 m ²)
Incidence Angle	0°	0°
Tail Arm	4.09 ft (1.25 m)	3.56 ft (1.08 m)

Figure 4.2: Tail Dimensions

Battery		Motor	
Model	AA Portable Power Corp. Hump Pack	Model	AXI 4130/20 Gold Line
Capacity	3800 mAh	Gearbox	Brushless
Voltage	18V	Power Rating	305 RPM/V
Cell Count	15	I_0	1.2 A @ 10 V
Pack Weight	1lbs 13 oz	Resistance	99 mohm
		Total Weight	.9 lbs
		Propeller	18 x 12

(a) Battery Dimensions

(b) Motor Dimensions

Figure 4.3: Battery and Motor Dimensions

4.2 Structural Characteristics

The main design criteria considered while designing the structure of the aircraft was the maximum loads the plane would experience during flight, landing, and tests during inspection. With that in mind, the team designed a strong but lightweight fuselage that could withstand impact on landing. Similarly, the wings were designed in such a way as to pass the structural test of picking the aircraft up by each wingtip. The wing loading during flight was also considered in order to ensure the aircraft's structure was sufficient for any worst case scenario. The results were a 0.9lb fuselage made mostly of balsa wood bulkheads and carbon fiber strings creating a total empty weight of 7.845 lb.

4.2.1 Fuselage

The fuselage, as shown in Figure 4.4, was designed to support the weight of the weight of the plane and in addition to the maximum payload it carries. It features stringers connected to a series of 10 bulkheads variably spaced to hold payloads and support aircraft structures, such as the tail and the motor. The stringers are 1/8" outer diameter carbon fiber rods that were connected to the fuselage using a combination of CA glue and Kevlar twine. Because the bulkheads vary in size, the stringers are bent into shape and are thus force-loaded, providing additional strength and stiffness of the airframe. The bulkheads were made out of either three or four 1/32" sheets of balsa wood with alternating grain orientation, thus

ensuring strength in all directions. Lightening holes were cut out of each bulkhead to reduce their weight.

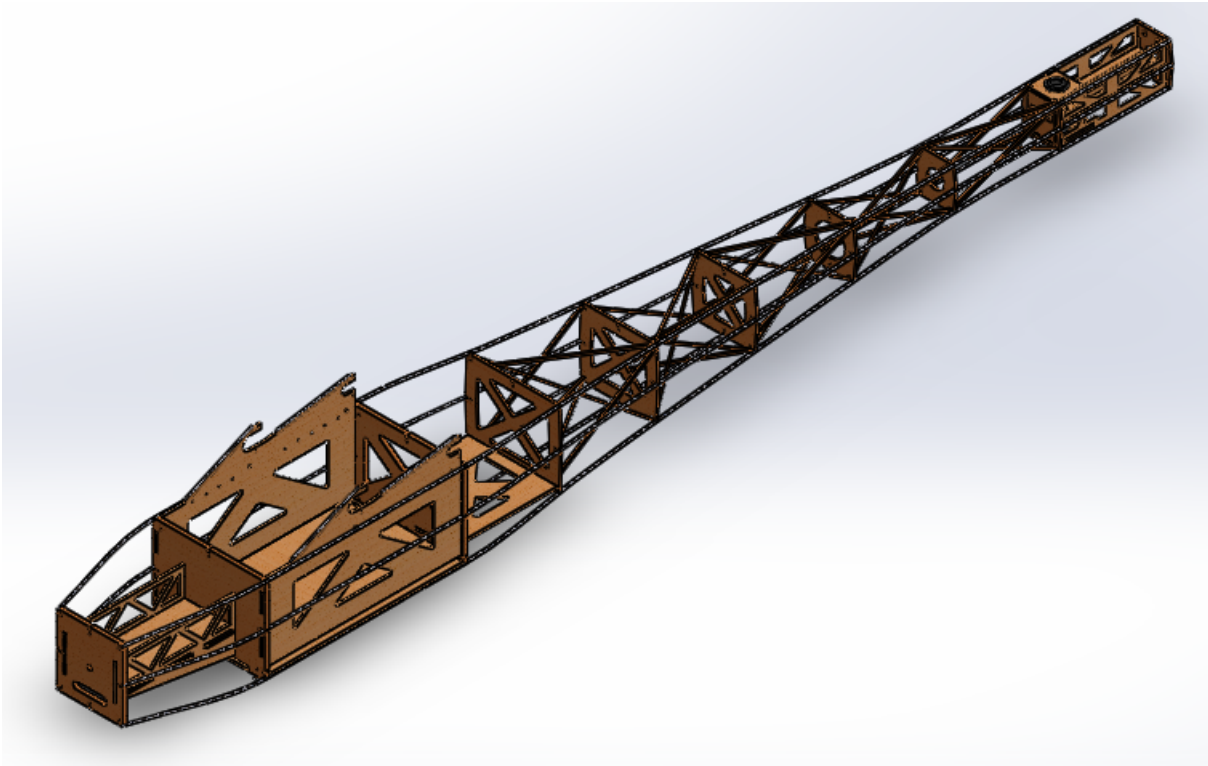


Figure 4.4: Fuselage Structure

The flooring and walls in the front of the fuselage were designed to hold the electrical components of the aircraft and were made from 1/16" basswood. These structures tab into both the bulkheads and each other for added strength and reduced flex. The basswood flooring located aft of the payload box was originally designed to provide a mounting plate for the dropping mechanism. However, though the team decided to attach the mechanism at a different location, this tabbed floor was kept as a structural member of the fuselage. The basswood tail box was designed in the same manner as the walls and flooring in the nose section of the aircraft, though the tail box was required to hold both the horizontal and vertical tail as well as two flight control servos.

4.3 Subsystems Design

4.3.1 Propulsion

Motor and Electronic Speed Controller Selection

In order to effectively complete all missions defined by the competition, a motor which could maintain high speed for short missions and comfortable speed for numerous laps was required. In order to gain a greater understanding of the motor size required, aircraft weight estimations were made. A table of these estimations can be found below with the maximum aircraft weight taken from the SolidWorks model.

Aircraft Component	Estimated Weight [lbs]
Battery	2
Mission 2 Payload	5
Control Devices	1
Aircraft Structure	6
Estimated Total	14
Calculated Total	12.307

Figure 4.5: Aircraft Weight Estimate

Therefore, the overall aircraft weight could be approximated as roughly 14 lbs. However, in our final design stages, a more accurate weight calculation from SolidWorks yielded 12.307 pounds, which was supported from weight testing manufactured parts.

From these estimations, motor selection tools provided by Hobby Express [1], a reputable R/C aircraft website, suggested three AXi Gold Line Motors. A table detailing the specifications that went into the final decision can be found below.

Battery Spec.	AXI 4130/20	AXI 5320/34	AXI 5325/16
Weight [lbs]	0.9017	1.0913	1.2688
Controller	77A	77A	90A
NiMH [Y/N]	Y	N	N
RPM/V	305	206	350
Max Aircraft Weight [lbs]	15.4324	16.5347	13.2277
Cost	\$179.99	\$279.99	\$299.99

Figure 4.6: Preliminary Motor Selection

The most important consideration when selecting the motor was its adaptability for a NiMH battery. It is clear that the only viable motor to select is the AXi 4130/20. Throughout the aircraft design process, a major effort was made to minimize aircraft weight. In choosing this motor, the aircraft would maximize its power-to-weight ratio by selecting the lightest motor.

The maximum aircraft weight allowable for this particular motor is approximately 15 pounds, leaving room for aircraft design and material changes. Additionally, the motor's specifications indicated a suggested electronic speed controller which was purchased alongside the motor. From the manufacturer's specifications, the eRC 85A SBEC electronic speed controller was purchased.

It was crucial to have an understanding of the motor's operating voltage in order to optimize the rated RPM/V in order to maximize the aircraft speed. However, due to the 2 lb. limitation placed on the battery, the most important task was to maximize power, ensuring sustainable high speed and long battery life.

Propeller Selection

The standard propeller for many large-scale R/C aircraft is the classic propeller configuration with two blades. According to the manufacturer specifications, AXi 4130/20 motor

called for an 18.5"x12" propeller. Due to the availability of propellers, an 18"x12" was purchased. The dimensions are in reference to the diameter of the propeller disc and the blade's pitch angle, respectively.

Battery Selection

After a few different attempts at finding a compatible battery for the selected motor had failed, the team decided to purchase separate cells of 1.2V NiMH batteries and manually connect twenty of them in series to create a 24V supply, the required voltage of the motor. However, most NiMH and NiCad batteries are not made for current loads of greater than approximately 7A while our motor required at least 15A. The team researched and found the Elite 2000 battery cell, offering 1.2V per cell and a 15-25A range while weighing just less than 1 oz. each.

Multiple methods to wire the cells together were attempted, but the final design involved each cell connected in series by soldering the battery terminals to strips of metal. The cells were also glued together with hot glue to keep its shape, wrapped in electrical tape on the top and bottom to cover any open terminals, and finally taped with packaging tape to hold it all together and pass the safety requirements of the competition. The final result was a homemade, NiMH battery rated for 24V, 2000 mAh, at a weight of 21 oz., well underneath the 32 oz. limit.

4.3.2 Controls

The receiver and transmitter were selected based on their fail safe mechanism. The Spektrum AR610 receiver has a built-in fail safe mechanism that cuts all power to the servos and sets the throttle to the low-setting that was selected during pairing to the receiver. The control surfaces are being set with the failsafe configuration as their no power state, causing them to revert back to this state if the power is cut to the servos. This allows the aircraft to meet the failsafe characteristics for the competition. The transmitter selected

was the Spektrum DX5E. The DX5E is a five channel transmitter that was recommended by Spektrum to pair with their AR610 receiver.

Servo selection was based on the size of the tail control surfaces. Due to the fact that both the vertical and horizontal stabilizers are full flying control surfaces, large forces are going to be exerted on the elevator and rudder, requiring strong servos to move them. High-torque servos were needed to meet the required forces necessary to move the surfaces, leading to the selection of the HI-TEC “HS-645MG” Ultra Torque.

4.3.3 Landing Gear

The landing gear configuration was based off of a traditional tail-dragger configuration. This configuration proved to be better suited for our aircraft due to the fact it is lighter and it creates less drag than a tricycle configuration.

The main gear, located just in front of the center of gravity, was initially chosen to be made from spring steel. A single spring steel rod was bent into a symmetrical bracket that extended out and back from our second bulkhead to place the wheels at roughly the center of gravity. It connected using brackets mounted to the bulkhead located 8.41 inches in front of the center of gravity, and extends until the wheels are 3.22 inches in front of the center of gravity. The bracket extended downward below the lowest point of the drop mechanism, creating a gap of 3.7 inches between the lowest point and the bottom of the wheels.

Upon preliminary flight testing, it was discovered that this main gear design caused structural failure in the foremost bulkhead and motor mount upon landing. The spring steel alone was not rigid enough to support the force of the landing impact, and the tensioning safety wire would tear the foremost bulkhead from the stringers. After repairing the damage and confirming the problem on a second flight test, the main gear was reconfigured using a 1/16th inch sheet 6061 aluminum. This was cut into a symmetrical strip with a rectangular center section and tapering outer sections, then bent into a trapezoidal shape. A spring steel axle connected the slotted tabs at the bottom of this aluminum gear to larger, 4.5 inch

wheels. Tensioned safety wire was again implemented to brace the sheet aluminum to the spring steel axle. An L-bracket was also installed in the forward corner of the main payload box, through which the new landing gear was bolted with some structural components added for further support and load distribution.

The rear wheel is attached via a spring steel rod that was bent to shape. The rod is held on by two small brackets that allow it to spin freely. A control tab was also connected to the spring steel rod, allowing it to be turned with the rudder, creating a steerable landing gear. The moving landing gear would have been much more difficult with a tricycle configuration, due to the distance between the servo and the moving wheel.

This landing gear configuration performed very well. It caused no damage to any components of the fuselage. Upon imperfect landings, the aluminum would crumple and absorb nearly all of the impact force. It could then be very easily bent back into shape in the field. This allowed the team to conduct multiple consecutive flight tests without needing to return to the lab to make repairs.

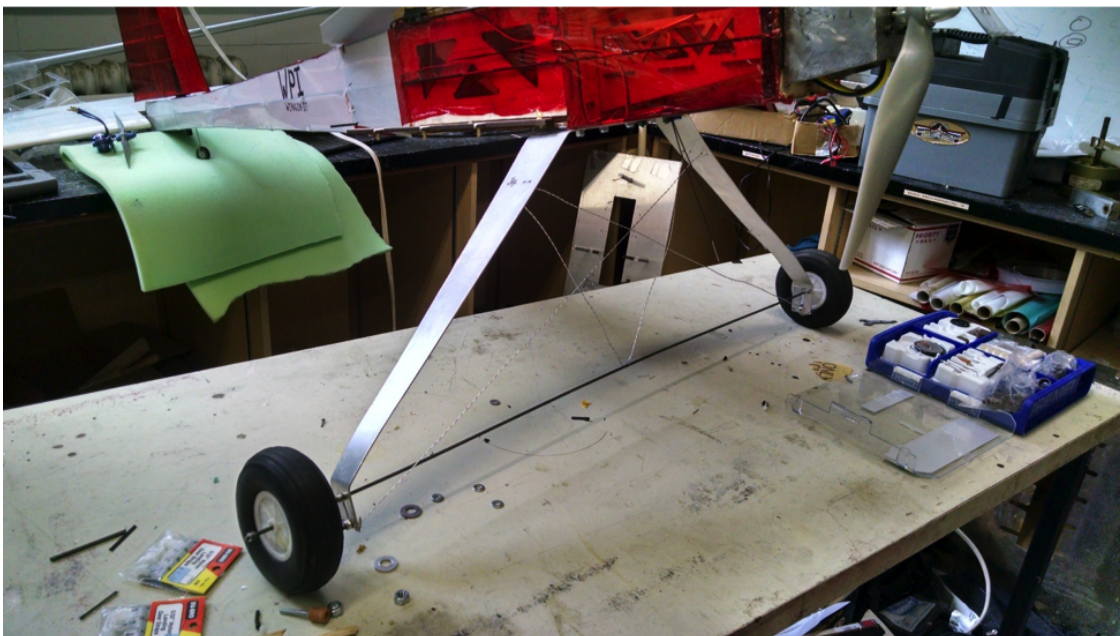


Figure 4.7: Final Landing Gear Configuration

4.3.4 Payload

For the ground mission and mission 2, the wooden block payload must be secured within the fuselage. The design of the fuselage was based around a space correctly sized for the block with a quick access opening under the wing. Due to the 1/8 inch tolerance on the block's sizing, extra space was added to the storage area to account for any increased size. In order to make sure the block will not slide within the fuselage during flight, Velcro is being used to secure it to the floor of the fuselage. 2 Velcro straps are going to be wrapped around the block itself, which will then stick to the Velcro strips attached to the floor of the fuselage. This will create a secure connection for the block and ensure that it does not move during flight.

4.3.5 Drop Mechanism

The final design of the drop mechanism utilizes the ratchet and camshaft combination, while taking up minimal space and being lightweight. The final design used the camshaft to actuate a series of lifters, similar to how an internal combustion engine actuates valve movement. The lifter arm is spring loaded, and secures a wire pin holding each whiffe ball to the exterior of the aircraft. The whiffe ball carrier consists of 7 wires secured to the wing with a hinge. The other end of the wire is pinned to the drop mechanism lifter on the fuselage at a 45 degree angle. These wires pass through the center axis of the balls. By doing this, the balls will remain in the same location if attached by only 2 points, thereby restricting their ability to move and interfere with other any part of the aircraft.

Each actuation of the mechanism causes one cam to push down on a lifter arm. The lifter arm then moves the wire pin, which uses gravity to swing free and allow the ball to drop clear of the aircraft. By using a centerline camshaft, which runs below the fuselage, we were able to split the ball distribution between the left and right side of the fuselage, contributing to a streamlined and compact design.

The servo, ratchet, camshaft, lifter series, and pin catches are all contained within a 6 inch by 16 inch carrier train system. This lifter training is connected to the bottom of the fuselage using pins held in tension with rubber bands. This make the entire mechanism easy to remove and very modular. The pins remain attached to the inner wing section, allowing the components to be easily separated and put into containers, which was key for shipping the aircraft to Arizona.

4.4 Weight & Balance

A weight and balance table is an extremely useful tool when designing an aircraft. It allows the design team to understand exactly where excess weight exists so that they can reduce weight in those areas. Additionally, knowing the aircraft's center of gravity is important for the stability analysis. This plane's center of gravity is forward of the aerodynamic center of the aircraft on every mission, thus ensuring stable flight and taxiing. All CG locations are measured from the tip of the propeller hub, which is the very front of the aircraft. Additionally, aircraft components will not change location between different missions. The weights of all components and their respective gravitational centers are detailed in Figure 4.8.

Component	Weight	CG Location			Static Margin
		X	Y	Z	X
	[lbs]	[in]	[in]	[in]	[% Chord]
Mission 1 - Empty Aircraft Total	7.845	15.819	0.008	0.978	4.474
Wing	2.452	17.839	0.000	4.129	-
Horizontal Tail	0.134	65.235	0.000	0.000	-
Vertical Tail	0.076	59.475	0.000	6.061	-
Fuselage	0.905	24.253	0.000	-0.595	-
Motor	0.922	2.431	0.000	0.000	-
Motor Mount	0.179	2.519	0.000	0.000	-
Propeller	0.190	0.977	0.000	0.000	-
Propeller Hub	0.030	0.530	0.000	0.000	-
Landing Gear (Front)	0.205	14.248	0.000	-4.949	-
Landing Gear (Rear)	0.030	58.083	-0.091	-1.941	-
Dropping Mechanism (Empty)	0.207	18.845	0.046	-3.648	-
Servos (Flight Control)	0.241	61.883	0.000	-0.279	-
Servo (Dropping Mechanism)	0.040	10.611	1.410	-3.070	-
Receiver	0.019	6.643	0.000	-1.000	-
Speed Controller	0.146	8.108	0.000		-
Battery (Motor)	1.800	8.108	0.000	-0.021	-
Battery (Servos)	0.270	9.198	0.000	-1.100	-
Mission 2 - Block Payload	12.845	16.321	0.005	0.622	3.707
Block Payload	5.000	17.108	0.000	0.063	-
Mission 3 - Bombing Run	8.423	16.028	0.057	0.938	4.165
Wiffle Balls	0.577	18.867	0.717	0.399	-

Figure 4.8: Weight and Balance

As seen in the above table, the empty weight of the aircraft is 7.845 pounds. This weight is relatively high for an RC aircraft, but for a 10-foot wingspan RC aircraft that can carry multiple payloads, the aircraft is has a low weight. Additionally, the aircraft center of gravity is located as close as possible to the quarter chord of the main wing. Though the CG is located slightly behind the quarter chord, the static margin is still favorable for stability in all missions. With the intention of not causing a massive shift to the overall center of gravity when the payload was added, the payload box was placed as close to the empty aircraft center of gravity as possible.

4.5 Performance Parameters

Performance Parameter	Mission 1	Mission 2	Mission 3
$C_{L,max}$	1.8	1.8	1.8
$C_{L,cruise}$	0.9	0.9	0.9
$C_{D,0}$	0.1027	0.1046	0.1439
L/D_{max}	10.9283	10.9283	10.9283
L/D_{cruise}	7.6475	7.3359	5.4925
Rate of Climb	10.07 ft/s	6.42 ft/s	7.64 ft/s
W/S [lb/ft. ²]	0.626	1.055	0.676
Cruise Speed	45 mph	35 mph	30 mph
Gross Weight	7.307 lbs.	12.307 lbs.	7.884 lbs
N_{laps}	4	4	7
W_{cargo}	N/A	5 lbs.	0.577 lbs.
Mission Score			

Figure 4.9: Performance Parameters

Manufacturing

5.1 Process and Techniques

We researched and implemented numerous processes while building our aircraft. These processes and techniques are described below.

5.1.1 Laser Cutting

Laser cutting was one of the most important processes for manufacturing the DBF aircraft. We used a VLS 64 laser cutter located in WPI's Washburn Shops. This laser cutter has 60 watts of cutting power and provides two-dimensional tolerances under 0.001 inches. This machine is capable of accurately cutting most plywood and acrylic under 0.375 inches very quickly.

The VLS 64 is driven by CAM software and interfaces with a computer much like a printer. The first step in producing any part using this process is to create a two-dimensional AutoCAD sketch. The user then uses the AutoCAD "print" feature to import the sketch into the CAM software for the laser cutter. Once the sketch is imported, the user can move the sketch within the cutting area and set appropriate cutting speed and power for the material.

The laser cutter will then follow the sketch exactly. It can cut 0.25 inch acrylic and balsa in a single pass, making the process very fast. The setup is also simple, as the CAM software automatically sets machining paths based on AutoCAD sketches with no additional user input.

This process has two main limitations. First, the VLS 64 is limited to cutting plastic, wood, and glass. It cannot cut fiberglass, carbon fiber, or any metals. Additionally, it is strictly a two-dimensional machining process. This means that all of the parts we create

using this process must be flat.

5.1.2 Balsa Ply Construction

Balsa wood is widely used for construction in model airplanes. It is light, has a good strength-to-weight ratio, and is inexpensive. Like all wood, it has a unidirectional grain. This means that it is strong in axial tension and compression applied parallel to the grain, and very strong in compression perpendicular to the grain. However, it is very weak in bending when a load is applied to a moment arm perpendicular to the grain. In order to counteract this problem for components subjected to high shear stresses in multiple directions, we created balsa plywood with alternating grain direction for each layer.

We created 0.125 inch ply from four layers of 0.03125 inch balsa sheet. We cut six by six inch square pieces of sheet and bonded them into a stack using wood glue. We pressed the pieces together until the glue was dry to prevent warping and ensure complete bonding. We alternated the grain direction for each layer in order to mitigate the problems described above. The resulting ply was significantly stronger when subjected to both normal and shear stresses than a single balsa sheet of the same thickness.

5.1.3 Carbon Fiber Tubing

Much of the structure of our aircraft consists of carbon fiber tubing. This tubing is extremely strong in tension, compression, bending, and torsion. It is also very rigid, which makes it an excellent choice for components with low tolerance for flexure (i.e. wing spars and fuselage stringers).

In order to create structure using these tubes, we needed to cut them to length and bond them to wooden substructures (i.e. ribs and fuselage bulkheads). We used a Dremel tool with a rotary cutoff head to cut the carbon fiber. This created a relatively clean cut with minimal material removal. However, it did create hazardous carbon fiber dust, so we wore dust masks and goggles when performing this operation. We used Cyanoacrylate glue to

bond the carbon fiber tubes to the balsa ribs and bulkheads.

5.1.4 Carbon Fiber Wet Laying

Carbon fabric is used in the D-cell component of the wing to provide strength to the leading edge and to prevent scalloping when the wing covering shrinks. The fabric is cut to size and then coated in an epoxy resin to turn the fabric into the hardened carbon fiber composite.

We used the wet laying process of forming carbon fiber to create our D-cell. The D-cell will be initially formed by soaking 0.0625 inch balsa in warm water to make it easy to bend and tacking it into the shape of the leading edge. The epoxy is painted onto the balsa to create a base coat for the fabric to stick to, and the fabric is then draped onto the balsa. More epoxy is spread onto the fabric to soak through it and further increase its bond to the balsa. Squeegees are then used to remove any excess epoxy from the surface. Peel ply, a nylon fabric sheet, is then laid over the fabric and squeegeed again. This sheet absorbs extra epoxy and can be peeled off the fabric after the resin has hardened; it also covers the fabric to protect it while it dries. After the fabric has hardened the peel ply is removed and the fabric will remain bonded to the balsa D-cell.



Figure 5.1: Wet Carbon Fiber

5.1.5 Sheet Metal Forming

The only metal part on our aircraft (the engine mount) was simple enough to be hand formed from sheet metal. To create this part, we cut it to shape using a rotary cutoff tool. We formed the geometry using a variety of tools, including the metal brake, drill, vice, hammer, and pliers.

5.1.6 Ultracoating

Ultracote is a thin plastic sheet that model aircraft builders use as covering fabric. This material is slightly thicker than typical plastic wrap and is adhesive on one side. It also shrinks when subjected to heat. This allows it to adhere to and tighten over wing and fuselage structures, creating a smooth surface finish. The process for applying ultracote is simple. It comes in large rolls, which can be cut to size based on the amount of surface area to be covered. Once the piece is cut, the protective layer is peeled off, exposing the adhesive surface. This surface is laid onto the structure and bonded by pressing with a pre-calibrated specialized iron. Once the ultracote is bonded to the structure, it can be heated until taut using a heat gun.



Figure 5.2: Coating the fuselage

5.2 Wing Construction

5.2.1 Wing sub-assemblies

The wing assembly was based around alignment with the two carbon fiber spar tubes that run the length of each section. A jig was created out of laser cut balsa wood, which held the spar tubes at the correct distance and at a height that would keep the ribs from touching the surface the jig was resting on. Ribs were slid onto the spars until they were at the correct distance from the next rib/end of the spar tube, as confirmed by measurements with calipers. Once all of the ribs were in their correct places they were glued into place with cyanoacrylate glue. The drawings in appendix A shows an exploded view of the wing assembly that was used to align the ribs.

The next step in the manufacturing of the wing sections is to attach the D-cell to each rib. The inner layer of the D-cell is made of 1/16 inch balsa wood, which is soaked in water to make it softer and flexed into the shape of the leading edge of the airfoil. The balsa is then pinned onto the ribs and a heat gun is used to speed up the drying process of the wood. Once the wood is dried it will then be glued into place with cyanoacrylate glue. Once the wooden D-cell is made, the carbon fiber layer will then be added to create a stronger and more rigid leading edge on the wing. The carbon fabric will be wet laid onto the wooden D-cell and left to cure as described in section 5.1.4.



Figure 5.3: D-cell forming.

Once the D-cell has been added, the outer wing sections and the outer portions of the middle section must be wrapped in ultracote. The ultracote is cut to size and attached to each wing section as described in section 5.1.6.

5.2.2 Dihedral Boxes

The dihedral boxes were assembled using the pieces of laser cut balsa and bass wood. The pieces have a system of tabs and slots that allow them to fit together and form a box with sets of holes for the spars to slide into. Once all of the pieces were fit together correctly,

the box was glued together using cyanoacrylate glue. Gussets were then fit into the box to increase strength and glued in place once they were properly aligned with the spar holes in the box.

Once the box and gussets were glued in place, strips of 1/16 balsa were laid on the top and bottom of the box between the airfoils to create a floor and roof for the box. The dihedral box was then wrapped in ultracote. The dihedral boxes were then used to attach the wing sections together using nylon nuts and bolts that fit into precut holes in the outer most ribs of each section of wing.

5.2.3 Thermoform Plastic Cover

A plastic cover was used to cover the center section of the wing where it meets the fuselage, to create better airflow over the top of the aircraft. A foam mold was cut to the shape of the upper surface of the airfoil using a hot wire cutter. This shape had a piece of heated thermoform plastic laid onto it, which will take its shape. This piece of plastic was trimmed to size using a knife and attached to the center wing section.

5.3 Fuselage Construction

The fuselage was constructed in three major steps. The first step was to create the bulkheads from plywood and compartment sections from bass wood. The sheets were cut and glued into three and four ply sheets with alternating grain to maximize strength while minimizing weight. The firewall was backed with a bass wood ply in addition to the balsa plywood to provide a stiff nut plate for mounting the motor mount. Each of these bulkheads along with the bass wood siding and reinforcement plating were then cut using a laser cutter. These sections were assembled using CA glue and interlocking tabs. Additionally, the wing attachment clip cradle was reinforced with carbon fiber tubes attached with a Kevlar wrap to help transfer the flight loads from the wing spars to the fuselage.

Once the box section compartments were assembled, they were placed on a jig. The jig squared each box section and independent bulkhead at their appropriate location in the fuselage. Step 2 began with wrapping 1/8" carbon fiber tubes from the front to rear of the fuselage using guides cut into the bulk heads. The tubes were glued into the slots, then fastened with a Kevlar wrap rib stitch to ensure they would not break free. Since each tube length was limited to 4 feet, the tubes needed to be sleeved and extended using 1/8" inner diameter brass tubes. After the initial gluing sequence, the fuselage was checked to ensure it was square.

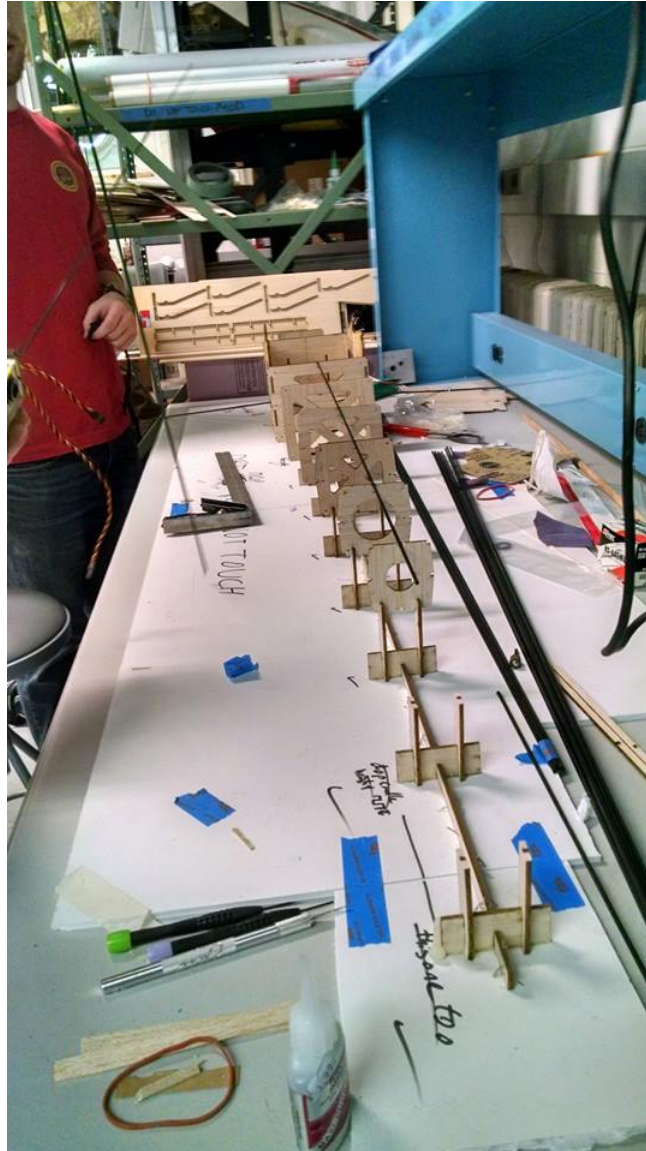


Figure 5.4: Fuselage Construction Process

Once the carbon fiber tubes were cured, and everything was squared, the final step began with the internal balsa wood trussing. Using 1/8th square stripes of balsa, the fuselage tail section was reinforced to counter any bending or twisting moments. This was accomplished by triangulating the each face of the tail box sections. Careful attention was paid to ensure that the tail remained within square during this process. Once completed, all minor attachment points were glued in place along with any electronics or special purpose fixtures. Finally, after all components were checked for adequate fit and control systems tests were

completed, the fuselage was covered in Ultracote, completing the fuselage assembly.

5.4 Electrical System

Due to difficult requirements necessary to meet competition regulations and requirements, the team was forced to create a homemade battery using single cells and wiring them together. The cells selected would meet the motor's requirements while being well underneath the 2 lb. battery limit, but it would require connecting 20 cells in series. Several approaches were taken to accomplish this task.

First, the team utilized simple, inexpensive plastic battery trays easily found at local stores. These trays were very effective in their purpose of holding the batteries in an orderly and efficient manner; however, they had to be connected to each other by soldering wires to the terminals which occasionally melted the plastic tray. The springs and wires used in the trays were also too small of a cross-sectional area to allow for the 15-25A to flow. Instead, this configuration only allowed for approximately 7A to flow which would not power the motor effectively.

The team then attempted to construct a custom battery tray out of laser cut bass wood and strips of metal glued to the wood casing. This method created a very well-organized battery setup and solved the conductivity problem. However, it was found that some sort of compressive force would be required on the cells to ensure constant, reliable connectivity and so the team continued working on new ideas.

After several attempts were not satisfactory, the team finally decided to solder the batteries to metal strips. To do this, small copper tubing that was purchased for the dropping mechanism was flattened with a hammer to create a highly conductive metal strip. That piece of copper was then soldered to the positive terminal of one battery cell and the negative terminal of another. Once there were two physically parallel rows of ten cells, all connected in series, the size, weight, voltage, and current ratings were all up to specifications. This

method of soldering, while dangerous to do, solved each of the previous problems such as low conductivity or a need for a spring-like mechanism to create pressure. This final product was then tested, modified as necessary, and inserted into the aircraft for the competition.

5.5 Manufacturing Gantt and Milestone Chart

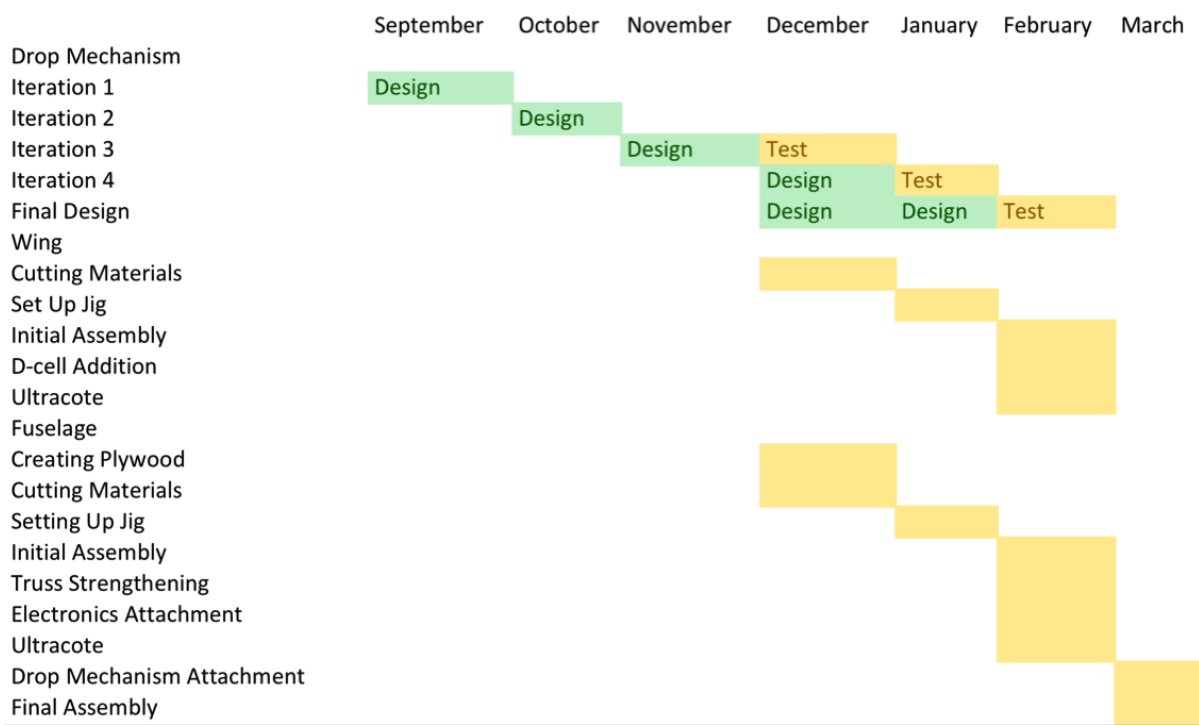


Figure 5.5: Manufacturing Gantt and Milestone Chart

Testing

The team conducted several tests regarding the structure of the aircraft, propulsion system, aerodynamics, and dropping mechanism. The main goals for these tests were to ensure structural integrity and fully functional components.

6.1 Flight Testing

The flight testing of the finished aircraft was conducted in 4 phases; Static testing, initial flight hops, initial flight test, and mission testing. Each test segment was designed to verify the function and performance of the aircraft in gradual steps. This allowed us to test the aircraft and identify problems while minimizing the risk of causing critical damage to the airframe. Throughout our testing we experienced a number of failures and successes that allowed us to tune our aircraft into a competitive product prior to attending the DBF competition.

6.1.1 Site location and Static Testing

The static testing, or bench testing, was designed to test all of the aircraft system to ensure they were free of defects that could result in a failure during the actual flight-testing. The initial tests verified the engine run time, servo function, wing strength and deflection, and drop test. The initial run test was conducted on the bench and consisted of running the experimental battery from a full charge to depletion. This test yielded an approximate run time of 11 minutes at 50% throttle on a full charge.

The next test we conducted was the final wing loading test. This was designed to verify that the wing could meet the required wing time loading requirements as defined by the competition. This test was conducted at the maximum mission gross weight and was passed

with flying colors. The wing faced a deflection of 7-8 inches at the wing tips without failure. The final bench test was the drop test. This test was devised to verify that the landing gear would be sufficient to withstand the forces of landing. For this test we dropped the unloaded fuselage from approximately 15 inches and experience no failures.

The final test, the servo deflection test, was conducted before each flight attempt. This involved simply checking each servo deflection to ensure all controls were deflecting with out error. This test saved the aircraft from what would have resulted in crashes on two occasions. On one occasion during flight testing the horizontal tail detached but was detected on the ground before the flight. Additionally, during competition, this test detected a faulty rudder connection. Dust had built up in the bearing causing a jam at full deflection. By conducting this test, we were able to avoid a crash.

6.1.2 Initial Flight Test hops

The initial flight tests were conducted to ensure several aspects of aircraft were in check before the aircraft flew. These flights were short hops flown 1-5 feet above the ground. The aircraft was taken off, flown shortly in a straight line, then landed, all within 100 yards. We conducted these flights on the WPI football field. The objective of these flights were to confirm all of the flight control were effective and trimmed correctly, to identify any short coming in the aircraft design, and test the take off and landing performances.

These flights quickly identified two issues; insufficient landing gear configuration and pitch control issues. The landing gear design was subject to failure due to the heavy weight of the aircraft and lack of sufficient structure supporting the gear struts. The 1/8th spring steel wire was to too thin to support the weight of the aircraft, and had to be braced with safety wire. The aircraft was never designed to accommodate the safety wire tie offs, which resulted in substantial damage during landings.



Figure 6.1: Damage Sustained during hops

The other issue was the small wheel diameter selected for the landing gear. The small wheel would rotate toe out on landing turning them into brakes. The sudden drag loads caused by the small wheels coupled with the safety wire design would transfer the landing loads to the front bulkhead. This in turn sheared the bulkhead from the aircraft. We attempted several reworks of the gear before the initial design had to be abandoned. A new rigid design with dedicated hard points provided us a much more durable solution. It was design with bungee shock absorption and flexible aluminum to absorb landing loads. If the design was overloaded, the gear legs would slowly collapse, minimizing the damage. We also increased the wheel diameter to 5 inches. The new landing gear worked well and proved to be reliable.

The only other issue to be identified during this flight testing phase was too much pitch control. When the aircraft was rotated, the aircraft would oscillate significantly due to Pilot Induced Oscillation (PIO). This is were the pitch authority exceeds the pilots ability to control it due to a response lag in the system, resulting in a growing oscillation in the

aircraft attitude. We adjusted the servos control throw on the servo arms and the transmitter, effectively eliminating this issue. Once we completed the ground flight tests we moved to the initial flight test.

6.1.3 Initial Flight Test

The initial flight test was conducted on the Wachusett Reservoir Dam. This area provided a clearing of 3000 ft. by 700 ft. as well as the full expanse of the reservoir itself. This provided us with adequate area to fly the aircraft. The initial flight test was carried out with a Lithium Polymer battery. While this battery would not be allowed for the competition, it allowed us plenty of power and duration to validate the entire flight envelope without having to worry about the experimental battery.

After checking all of the systems and center of gravity location, we simply accelerated the aircraft and rotated for a picture perfect takeoff. Right from the start it was clear that the aircraft performed very well. We conducted a series of gentle turns proving that the dihedral effect was indeed sufficient for all of our needed maneuvers. We also took this opportunity to practice some stalls to establish an approach speed for landing. Once we were happy with the flight parameters, we landed. During the second flight of the day we were able to verify all of the parameters from the previous flight. However, when turning final for landing, we entered a low altitude spin stall resulting in a crash.

The landing gear absorbed the brunt of the crash, which also lightly damaged 2 ribs and the motor mount. The damage was quickly repaired. Once the initial flight parameters were established and verified, we were confident the aircraft could sufficiently carry the block.

6.1.4 Mission Flight Testing

Once the damage from the initial flight-testing phase was fixed, we immediately moved to mission 2 flight testing, the payload mission. If the aircraft could not take off in the prescribed distance (60 ft.), then we would not qualify for the competition. For this test, we

installed the block payload, and flew the aircraft on a calm day. The first flight-tested the take off, climb and maneuver performance of the aircraft at gross weight. The aircraft flew for 12 minutes and landed safely.

Due to the heavy loading of the aircraft, it was important to verify that the aircraft would not fail due increased flight loads. To test this, we flew the aircraft at gross weight through a series of maneuvers. These maneuver included: steep turns, dives, power on and power off stall, chandelles , wing overs and high speed passes. Throughout all of these maneuvers the aircraft remained predictable and structurally sound.

Through the remainder of flight-testing, we experienced one substantial crash. This was caused by a broken elevator hinge, which resulted in the loss of pitch control. After a series of dramatics oscillations the aircraft was landed off field with minimal damage the landing gear. The aircraft was quickly repaired and returned to light.



Figure 6.2: Test Flight

Due to the lack of time, this concluded our pre competition flight testing. The aircraft had proven itself through an extensive series of gross weight flights. These flights validated the flight envelope as well as provided practice for the pilot. The time constraint did not permit us to test the drop mechanism or experimental battery, but both were proven on the

bench. With the conclusion of these tests we were confident that the aircraft would be able to perform all of the competition missions with a reasonable degree of confidence.

6.2 Drop Mechanism Testing

In order to make sure the drop mechanism worked correctly, two separate tests were run to see its performance on the ground. On the ground the mechanism was set up and properly wired, and actuated multiple times. This was to test the mechanism's ability to properly drop the whiffle balls one at a time without running into problems with the wire clips or the ratchet.

6.3 Structural Tests

The structure of the aircraft was examined in various ways. This included wing loading tests— especially on the dihedral boxes— fuselage loading and twisting, and landing gear tests to ensure propeller clearance in all practical situations. A basic torsional test was accomplished on the fuselage which was very encouraging as the structure proved to be very rigid. The aircraft was also put through a static load test by lifting the aircraft by the wing-to-fuselage attachment point hooks directly and by the entire wing with the payload inserted. A torsional test was also done by hand on a wing section by twisting the front and rear spars until failure. Another wing test was done to examine the strength of the dihedral boxes by increasing loads on the box while securing the two adjacent wing sections. Finally, the landing gear components also experienced simple tests to ensure strength and flexibility needed for distributing loads on impact.



Figure 6.3: Structural Test

6.4 Aerodynamic & Propulsion Tests

Mathematical examinations of the aerodynamics confirmed a stable aircraft both statically and dynamically. As previously described, the team verified the aircraft's stability in more detail during flight testing, which supported these calculations. Under ideal conditions, the propulsion system provided more than enough thrust to maintain proper flight speed and maneuverability during all three flight mission specifications.

6.5 Controls & Avionics

The controls and avionics underwent testing to check for any faulty wires or connection problems. For the first test the team connected all of the electronic components to the receiver and battery system. The transmitter was then turned on and each system was controlled one by one to ensure that each part of the system works. This test shows that all of the wiring is correctly done and that each servo and the speed control are all properly functioning.

The second test checked the range of the system. The system was turned on and one

team member constantly moved one control surface on the transmitter. That team member walked farther away from the receiver until the connection was lost. That distance was the maximum range for the transmitter/receiver system. Each component of the electronics system was tested at this distance to ensure that they all function properly when far away from the transmitter.

6.6 Battery Tests

In order to confirm the theoretical success of the homemade NiMH battery pack, the team tested capabilities. Using an inductive ammeter, the large current output of approximately 24.6A was measured. The soldered battery pack performed its max current test successfully and then was tested for lifespan. Running the motor up to approximately cruise velocity, the battery lasted for a total of 18 minutes on the first test. However, that includes a few minutes of significantly lower thrust output. The battery was tested again at a later time and supplied approximately 11 minutes of thrust roughly equivalent to that necessary for cruise velocity. These results were very encouraging as the expected lifetime value was only six minutes.

During all of these tests, the results seemed to show that each of the two homemade battery packs would work successfully. One problem occasionally arose when some of the solder would detach from a battery since the battery terminal's surface did not grip solder very effectively. Another concern was the temperature of the batteries as they ran the motor and as they charged, but these specific cells were designed to operate at high temperature and high current conditions so the team decided to move on as this was clearly the best option to this point. Overall, the testing was very successful in proving that the battery could supply enough current for a long enough time to fly each of the missions.

Performance Results

This section discusses the results of the previously described tests that have been run so far. These results were used to verify predictions made with different components of the aircraft and led to slight changes in material selections and design.

7.1 Structural Tests

7.1.1 Wing Torsion Test

The wing torsion test was used to show where the wing would break if exposed to high levels of torsion. This test caused a wing test section to break along the connection to the rear spar, showing that connection as the weakest point on the wing. However, a large amount of force was required to cause this failure and verified that we did not need any further trussing in the front of the wing as it did not fail near the leading edge.

7.1.2 Static Load Test

The initial static load test was used to verify that the wing connection points were strong enough to support the full weight of the aircraft during flight. When the aircraft was fully loaded, the center wing section was used to lift the aircraft off of the ground. This test did not break the wing connection points and verified that they are strong enough to hold the aircraft together during flight.

The wing tip test required by competition rules was conducted alongside during the flight testing phase. The purpose of the test was to ensure the structural integrity of the wing and its fasteners during the maximum wing loading. It required that, with the five pound

payload installed, the wing remain intact while being lifted from the ground by the wing tips at the chord location of the center of gravity. The dihedral boxes, which were the weakest points in the wing under tip loading, allowed for a significant deflection angle but did not fail structurally. As a result, the team was able to pass this requirement.



Figure 7.1: Static Load test during flight testing.

7.1.3 Dihedral Box Test

The dihedral box test was used to verify that the outer sections of the wing would remain attached to the center wing section when under static loading equal to the maximum weight of the aircraft. When this test was performed, one of the dihedral boxes cracked near the inner ribs at the point where the angle changes. This led to the bass wood thickness being increased to 3/16 inch from the initial 1/8 inch for added strength.

7.1.4 Landing Gear Weight Test

The landing gear test was used to ensure propeller clearance when on the ground and that the landing gear would remain rigid enough to have a safe landing. When the landing gear was properly aligned with the second bulkhead and the wheels were attached, the propeller had clearance to the ground, verifying that the landing gear is properly shaped. The plane was then fully loaded, which caused the landing gear to over flex and the fuselage to touch the ground. This led to a slight design change in the front portion of the landing gear, where

a set of wires run to the front most bulkhead and between the legs of the landing gear. These wires will fight flex within the spring steel and create a stronger landing gear.

7.1.5 Fuselage Twist Test

The fuselage twist test was used to show that the fuselage would need increased trussing to supplement the bulkhead and stringer combination. The front of the fuselage was held in place while the tail section was turned and flexed. The fuselage flexed much more than expected and showed that there was weakness within the structure. This led to balsa wood strips being glued in between the bulkheads to create a truss system, which made the fuselage much more rigid and strong.

7.2 Controls Test

The initial controls test of the entire system was used to verify that every component of the electronics system worked correctly. Once the system was fully connected, each component was actuated one at a time. All of the servos and the motor with speed control worked correctly, which verified that the entire electronics system is correctly wired and fully functioning.

7.3 Competition Results

The AIAA DBF competition in Tucson, Arizona was attended on April 10th-12th by four members of the team: Andrew Andraka, Dan Cashman, Zach Demers, and Malick Kelly. These members at the competition, all dressed in WPI polo shirts as team uniforms, are pictured below. Out of the 100 teams that entered the competition, only 84 were able to enter competition reports by the specified date. Of these remaining 84, almost all teams sent a team to the competition at Timpa Airfield, a remote location roughly 45 minutes outside

of Tucson.



Figure 7.2: Malick, Andrew, Zach, and Dan at the DBF Competition

WPI's team, named "Wingin' It," was able to successfully complete the ground loading mission and flight mission 1. The plane was able to take off and land in the specified areas, and it handled well even in strong, variable winds without the 5 lb block payload. Additionally, the aircraft was able to take off and land successfully with the 5 lb payload for mission 2. Unfortunately, however, the plane was not able to complete flight mission 2 correctly due to a fried battery cell. The team's pilot, Andrew Andraka, noticed a steady decline in the power being outputted to the motor while the plane was completing the third and final lap of flight mission 2. Although the battery pack was not able to provide enough power to complete the mission, Andrew was able to land the plane safely in the field without any structural damage. This resulted in a zero score for that mission.

After the initial failure of flight mission 2, the team endeavored to refit the plane with a proper power supply and motor combination. Because the team brought two battery packs to Tucson, the back-up pack was tried next. However, before the next flight attempt, the cells of the backup battery began to burst in Zach's hand due to overheating in the Arizona desert. This pack was given to competition authorities for proper disposal. Next,

the team located the fried cell in the first battery pack and removed it. A single replacement cell was left over from manufacturing the packs, so it was used in place of the fried cell. However, even with this new cell replacing the damaged one, the battery pack was unable to supply adequate power to the motor for flight with the block. A smaller motor and propeller combination was used with this battery pack in hopes of getting more drain time out of the pack by using lower amperage, but this combination was also not able to lift the plane off the ground with the block. Due to time constraints at the competition, that was the final flight attempt undergone by WPI's flight team.

Although WPI was not able to fully complete flight missions 2 and 3, their performance on the ground mission and flight mission 1 earned the team a final ranking of 53rd overall. Additionally, the aircraft did not sustain structural damage at any point in the competition. This is more than can be said for a number of competing aircraft from other teams, many of whom suffered catastrophic failure.

Recommendations for future work

As the first team from WPI to enter the AIAA Design, Build, Fly competition, the team faced numerous problems and hardships that could have been easily overcome by taking easy, precautionary steps. The experience throughout the entire design, manufacturing, and testing process lead to the following recommendations:

First, it is vital to maximize the use of time dedicated to MQP. Making advancements early in the academic year will shed light onto future problems and alleviate the stress of encountering problems as the competition approaches. If possible, develop prototypes early in the year in order to more easily correct for any issues and tackle competition-specific complications.

Carefully study the competition rules and regulations. There are often very specific rules that apply to the competition (battery type, weight limitations, etc.) that can be easily overlooked which could cause disqualification.

In addition to the separation of specific teams (i.e. propulsion and aerodynamics, etc.) the overall team should designate a project manager. Ideally, the project manager will have prior R/C aircraft experience in order to properly guide the team towards success. The project manager's primary roles will include designating hard deadlines, facilitating product testing, and managing a team budget.

This year, no concrete budgeting system was used, but it would have been very useful. Implementation of a budget and utilizing an overseer will eliminate excessive spending. Parts and materials were often needed for new developments and after crashes, but it became difficult with a depleting budget. Managing the team's funds will ensure the highest quality plane to be built while ensuring financial stability.

In order to expand the working budget for the team, external sponsorship should be

obtained. The DBF competition allows for outside funding from sponsorship which will aid in producing the highest quality plane possible. The overall cost of the project will likely exceed initial estimates due to numerous prototypes, extra materials, unexpected failures, travel expenses, etc. This external sponsorship will alleviate the stress and worry of needing to purchase anything out-of-pocket.

Manufacturing and testing should be completed in parallel. One major issue that continuously slowed the overall process were “unknown-unknowns.” Parts were often manufactured or purchased and put aside in order to continue manufacturing. These unknown-unknowns often presented themselves with failures (i.e. landing gear configuration) which halted team progress. By manufacturing and testing individual parts, earlier, large and complicated changes/improvements will not need to be made so close to the competition.

Design for manufacturability and crash-resistant aircraft components. For example, the implementation of a full-flying tail and elimination of ailerons proved to be very successful. This was not only successful in optimizing our score, but by using a full flying tail instead of standard elevator and rudders, the tail was much more easily manufactured. In terms of crash-resistance, the hook and rubber band method for wing attachment proved very effective in crashing. During the airplane’s worst crash, the wing survived the crash by springing back, only suffering the loss of a few ribs.

Flight testing is a crucial component to success in the competition. First, the designated pilot will need numerous hours to acclimate himself with the specifically designed plane in order to maximize control and understand its limits. Additionally, using an easily accessible flight testing area is necessary. The team found, via Google Maps, and utilized an open field near the Wachusett Reservoir. The closest address to this location is 60 W Bolyston St. Sterling, MA. This field proved to be a very accessible and legal location for flight testing.

Lastly, perform propulsion/electronic system tests early and often. The main downfall at the competition was the failure of the battery-pack. It is crucial to ensure that a reliable battery is purchased or manufactured. If the budget allows, prepare numerous sets of

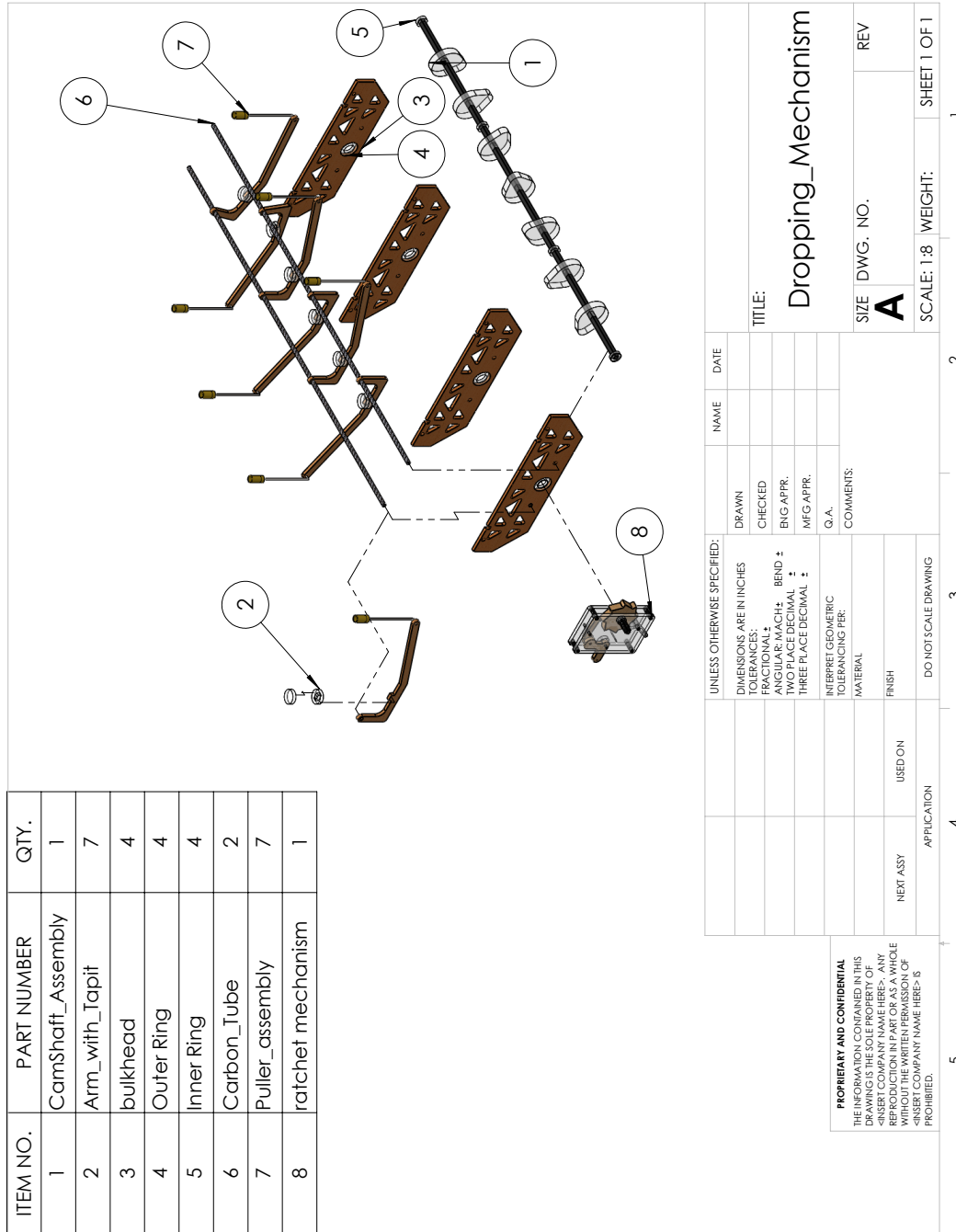
batteries in the event of a failure.

If these recommendations are taken into consideration, future teams will likely be able to avoid numerous issues that were faced. These recommendations will help eliminate unnecessary problems and expedite the entire aircraft design and manufacturing processes to ensure future success at the Design, Build, Fly competition.

References

- [1] *HobbyExpress.com: Radio Controlled Planes, RC Helicopters, & Cars Website*, September 2014 - April 2015. <http://www.hobbyexpress.com/>
- [2] *MATLAB & Simulink Student Version*. Computer Software. Natick, MA: MathWorks (2014). http://www.mathworks.com/academia/student_version/
- [3] Napolitano, Marcello. *Aircraft Dynamics: From Modeling to Simulation*, Hoboken, NJ: J. Wiley & Sons (2011).
- [4] Raymer, Daniel. *Aircraft Design: A Conceptual Approach*, 5 ed, AIAA (2012).
- [5] *RCgroups.com: The ABCs of Radio Control Website*, September 2014 - April 2015. <http://www.rcgroups.com/forums/index.php>
- [6] *XFLR5 Computer Software*. (2014). <http://www.xflr5.com/xflr5.htm>

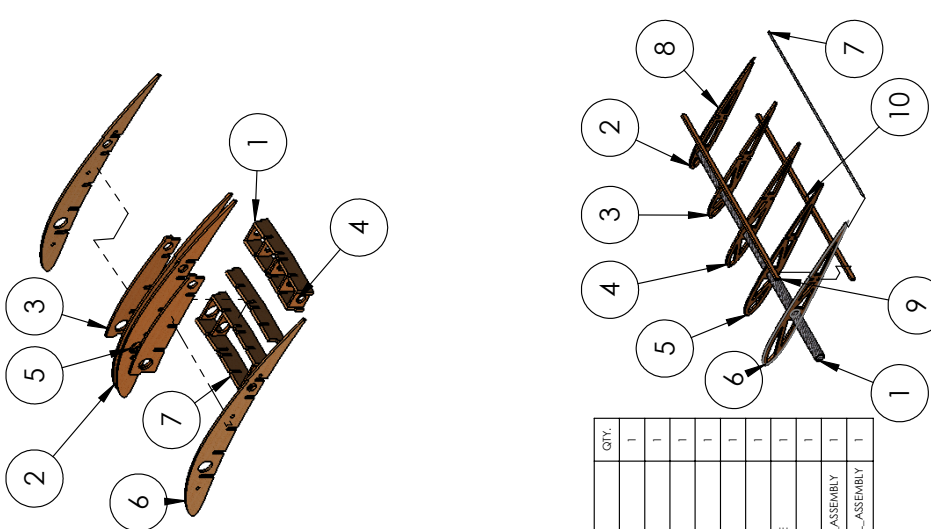
Appendix A. Drawing Package

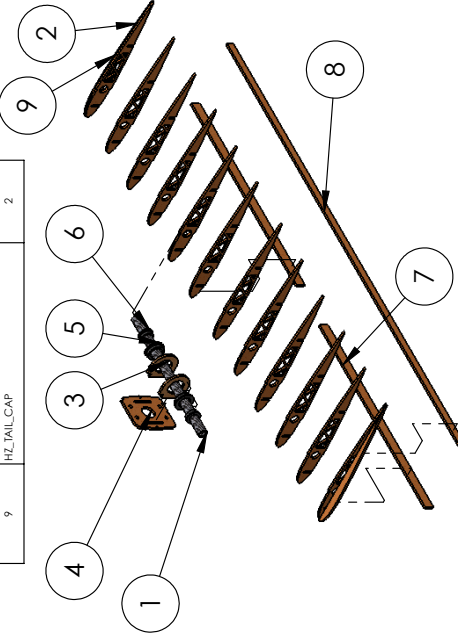


ITEM NO.	PART NUMBER	QTY.
1	Dihedral_Guide	4
2	NEW_DIHEDRAL_CROSS_MEMBER	2
3	DIHEDRAL_CROSS_MEMBER_MIDDLE	2
4	DIHEDRAL_COUNTERRAIN_PLATE	6
5	DIHEDRAL_COUNTERRAIN_PLATE_BIG	6
6	DIHEDRAL_RB_INNER	2
7	Dihedral_Guide_TAIL	1

ITEM NO.	PART NUMBER	QTY.
1	Tail_Spot_Main	1
2	Tail_Rib_mcd0012_TUBULAR	12
3	HZ_TAIL_TAB	2
4	BULKHEAD_HZ_CONNECTOR	1
5	VERTICAL_TAIL_BUSHING_OUTER	2
6	VERTICAL_TAIL_BUSHING	2
7	HZ_TAIL_BEAM_FRONT	2
8	HZ_TAIL_BEAM_REAR	1
9	HZ_TAIL_CAP	2

ITEM NO.	PART NUMBER	QTY.
1	VERTICAL_TAIL_SPAR_MAIN	1
2	5	1
3	4	1
4	3	1
5	2	1
6	1	1
7	VERTICAL_TAIL_TRAILING_EDGE	1
8	VERTICAL_TAIL_CAP	1
9	vf_beam (left)/VERTICAL_TAIL_ASSEMBLY	1
10	vt_beam (right)/VERTICAL_TAIL_ASSEMBLY	1

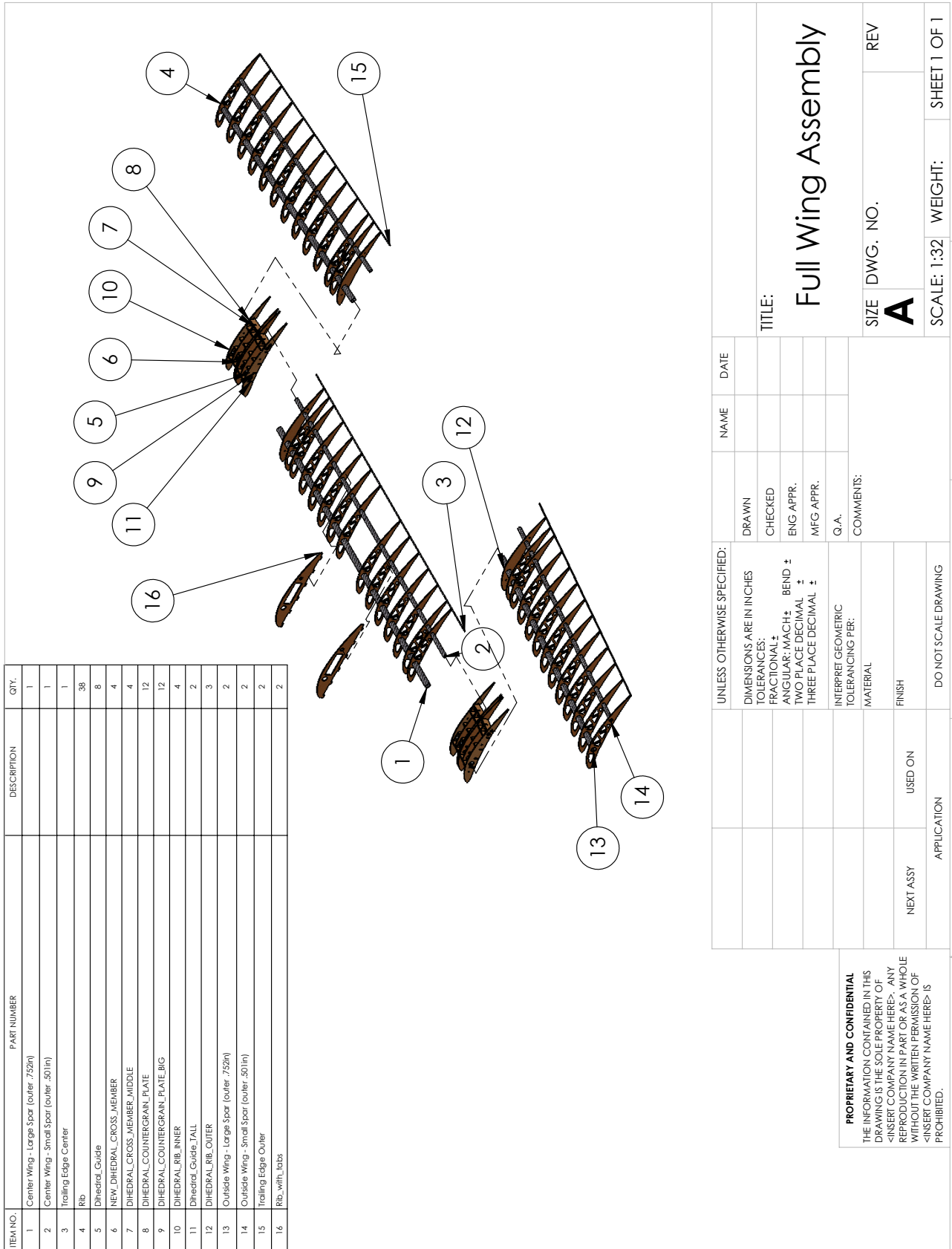




UNLESS OTHERWISE SPECIFIED:	NAME	DATE
DIMENSIONS ARE IN INCHES	DRAWN	
TOLERANCES:	CHECKED	
FRACTIONAL: ±	ENG APPR.	
ANGULAR: MACH: ±	MFG APPR.	
TWO PLACE DECIMAL: ±	Q.A.	
THREE PLACE DECIMAL: ±	COMMENTS:	
INTERPRET GEOMETRIC TOLERANCING PER:		
MATERIAL		
FINISH		
NEXT ASSY	USED ON	
APPLICATION		

SIZE	DWG. NO.	REV
A		
SCALE: 1:8	WEIGHT:	SHEET 1 OF 1

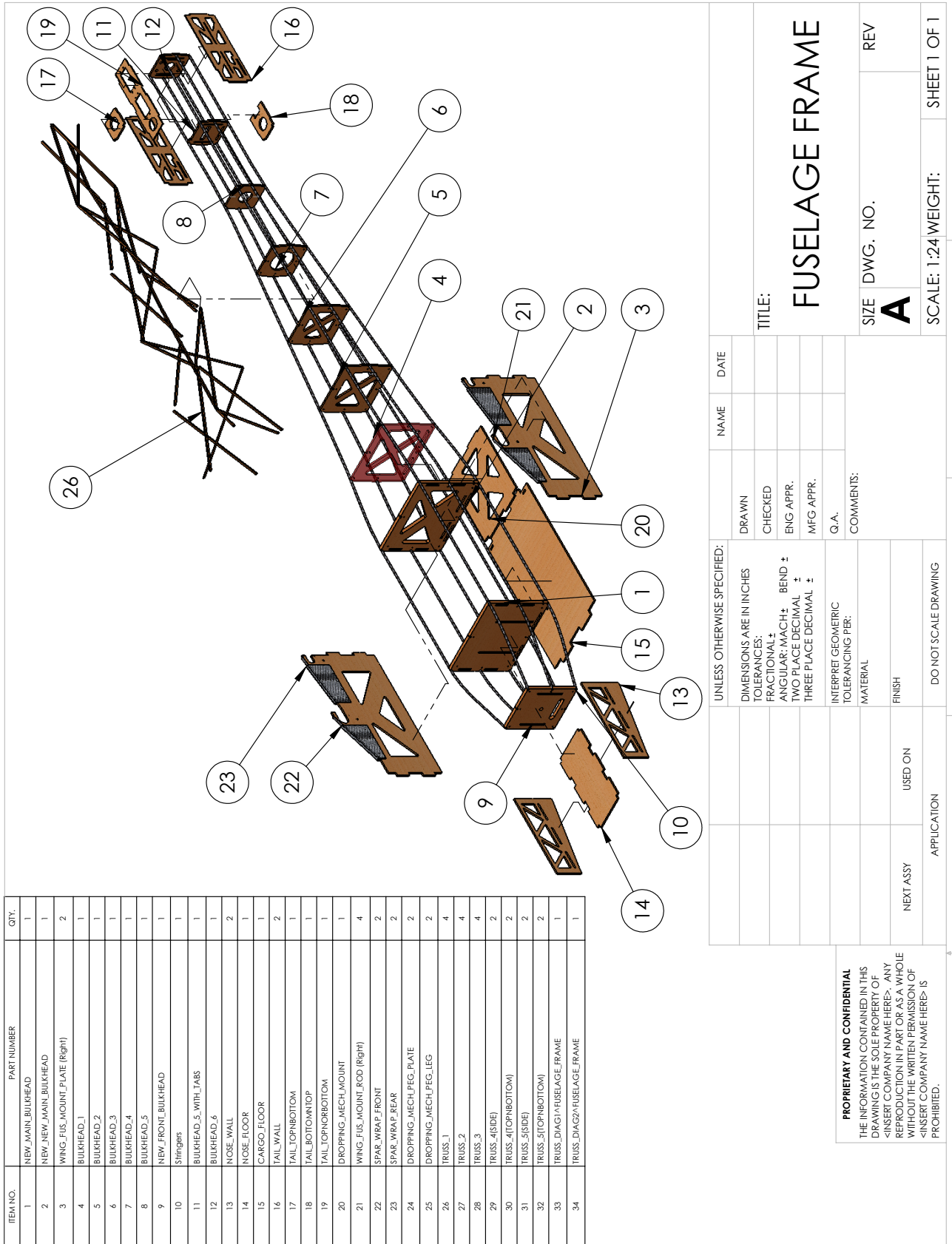
PROPRIETARY AND CONFIDENTIAL
THE INFORMATION CONTAINED IN THIS DRAWING IS THE SOLE PROPERTY OF <INSERT COMPANY NAME HERE>. ANY REPRODUCTION IN PART OR AS A WHOLE WITHOUT THE WRITTEN PERMISSION OF <INSERT COMPANY NAME HERE> IS PROHIBITED.

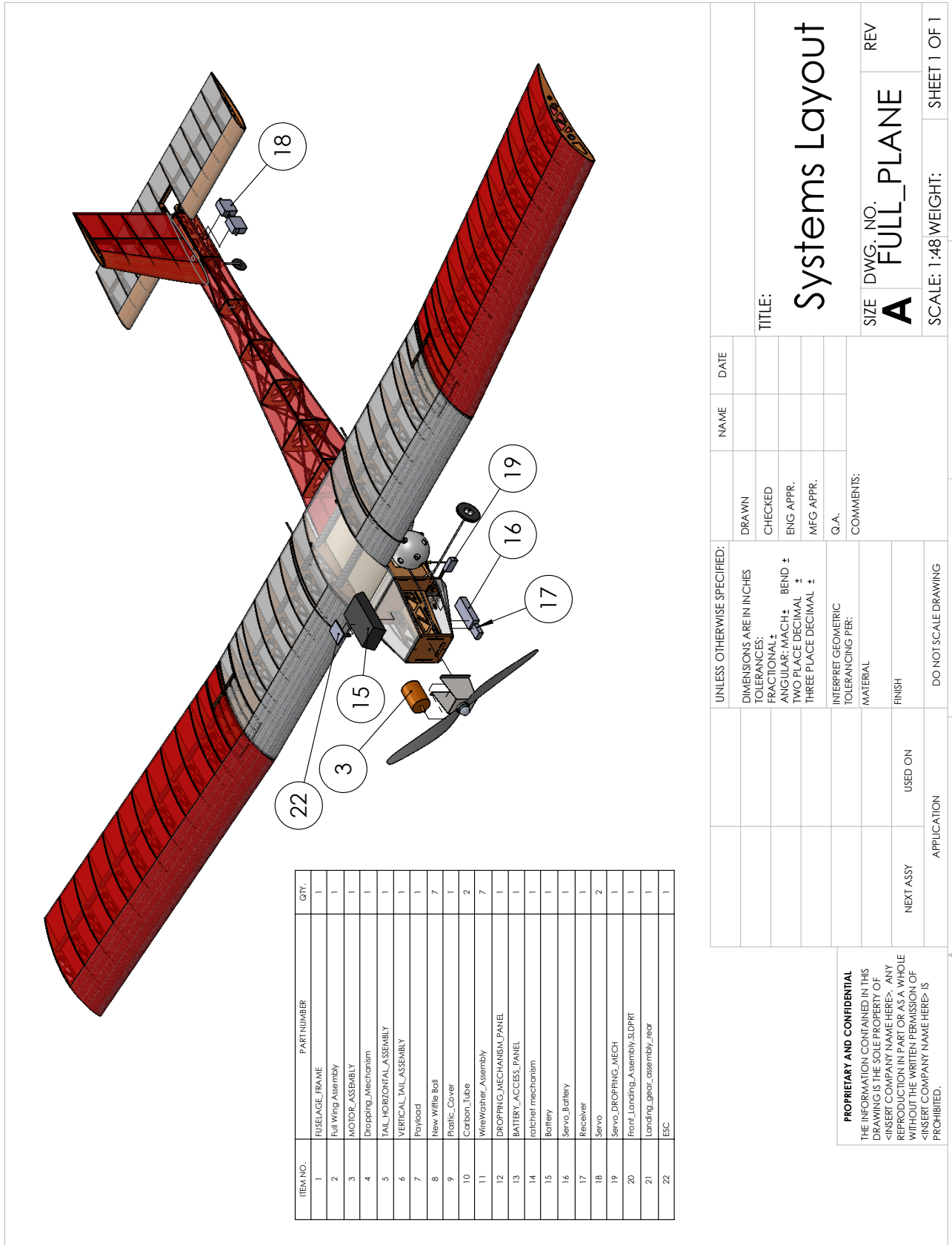


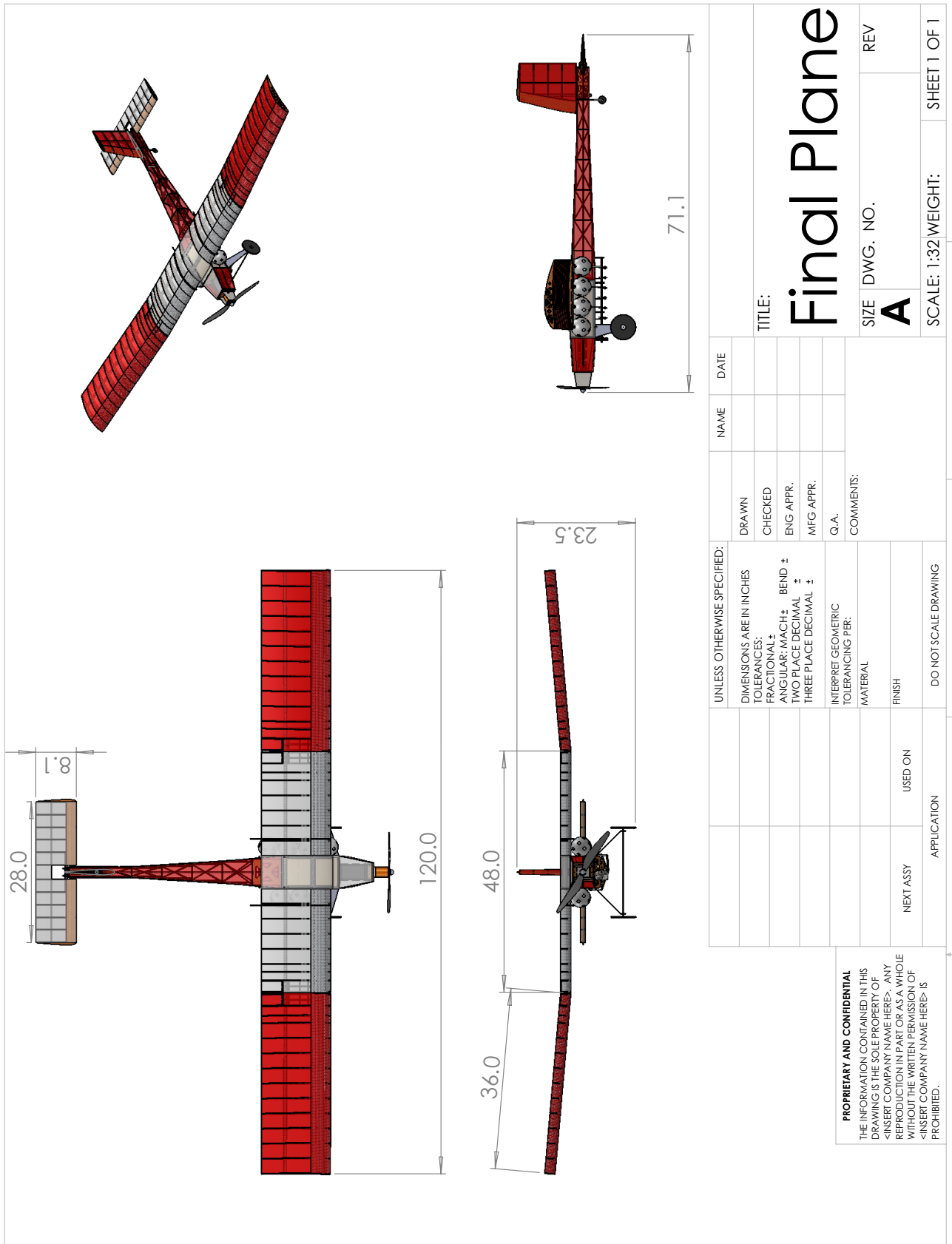
UNLESS OTHERWISE SPECIFIED:		NAME	DATE
DIMENSIONS ARE IN INCHES		DRAWN	
TOLERANCES:		CHECKED	
FRACTIONAL: ±		ENG APPR.	
ANGULAR: MACH: ± BEND: ±		MFG APPR.	
TWO PLACE DECIMAL: ±		Q.A.	
THREE PLACE DECIMAL: ±		COMMENTS:	
INTERPRET GEOMETRIC TOLERANCING PER:			
MATERIAL			
FINISH			
NEXT ASSY		USED ON	
APPLICATION		DO NOT SCALE DRAWING	

PROPRIETARY AND CONFIDENTIAL
 THE INFORMATION CONTAINED IN THIS DRAWING IS THE SOLE PROPERTY OF <INSERT COMPANY NAME HERE>. ANY REPRODUCTION IN PART OR AS A WHOLE WITHOUT THE WRITTEN PERMISSION OF <INSERT COMPANY NAME HERE> IS PROHIBITED.

TITLE: **Full Wing Assembly**
 SIZE: **A** DWG. NO.: _____ REV _____
 SCALE: 1:32 WEIGHT: _____ SHEET 1 OF 1







Appendix B. Org Chart

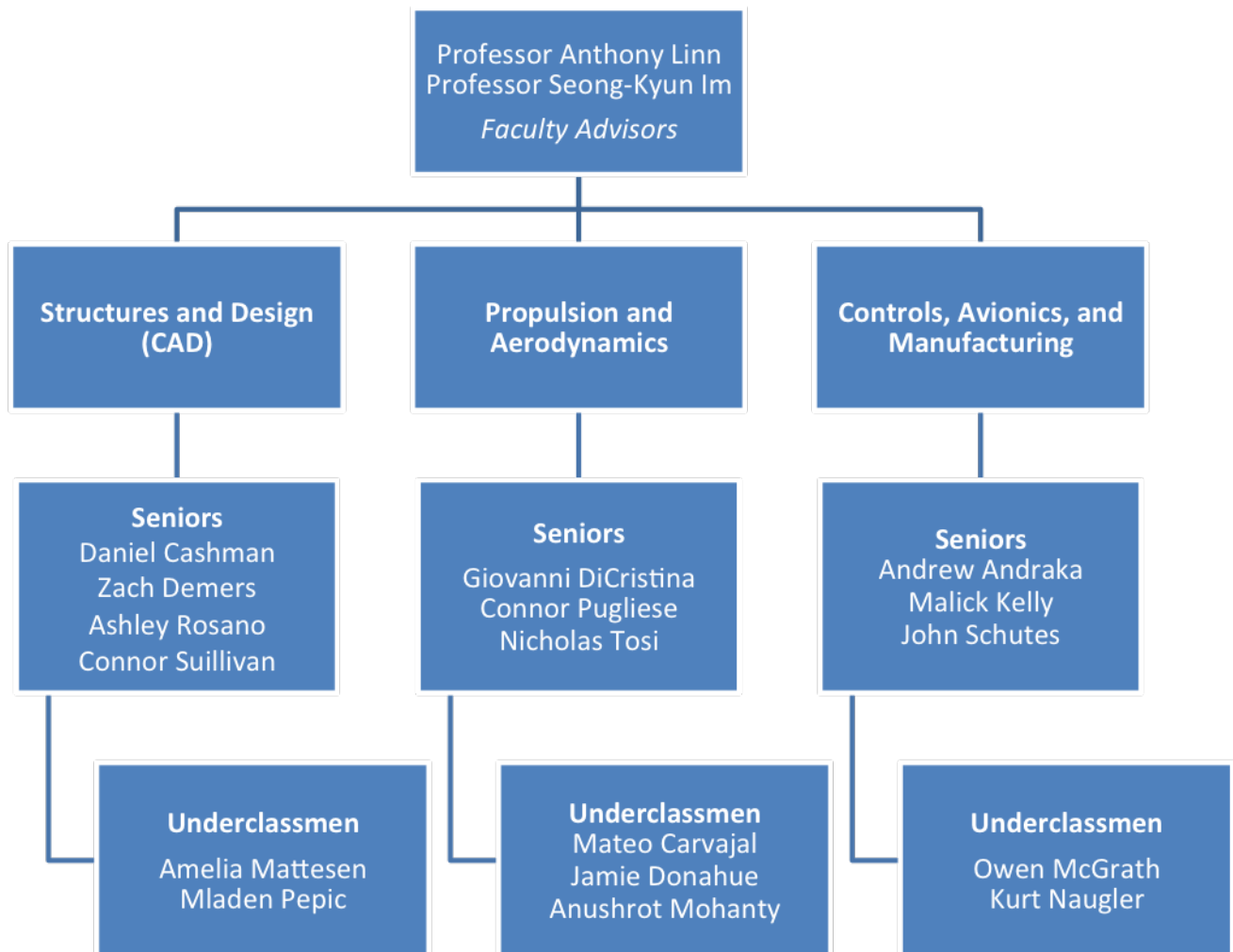


Figure B.1: Team Organizational Chart